PhD Thesis

Wound healing dynamics through the use of deproteinized bovine bone mineral (DBBM) and a porcine-derived collagen membrane in lateral bone augmentation. An experimental in vivo study in the beagle dog.

Chapter one

Introduction

Over the past few decades there has been an important reduction in the prevalence of tooth loss in many developed countries (Mojon *et al*., 2004). At the same time, we have also seen patients' life expectancy increase, as well as their demand for fixed restoration instead of removable prosthesis (Preciado *et al*., 2012; Oh *et al*., 2014). These changes have resulted in a shift in dental care towards other types of restorative and prosthodontics treatments rather than partial or complete removable dentures. Oral implantology is now a leading therapeutic solution for replacing missing or hopeless teeth. Fixed dental prostheses anchored by osteointegrated titanium fixtures can successfully remedy partial or complete edentulism, with a high survival rate in long term follow-ups (Albrektsson *et al*., 1986; Ekelund *et al*., 2003; Lekholm *et al*., 2006; Pjetursson *et al*., 2012). Implant surgery requires a complete diagnosis of the local and systemic conditions of the patient, which should include the medical history, physical examination and other diagnostic tests (e.g. radiologic or laboratory exams) (Eckert & Laney, 1989; Zitzmann *et al*., 2008). In this way, it is possible to optimize implant installation, which is a key factor for the aesthetic and functional treatment success.

Implant treatment plan with insufficient bone volume.

One of the factors for the success of an implant therapy treatment, is the amount of bone in the jaw. Having a sufficient amount of bone allows a prosthetically driven ideal three-dimensional position

of the fixture in the oral cavity. This requirement, however, is seldom met since even in healthy healed residual alveolar ridges, there has been a significant amount of physiological bone remodelling(Araújo & Lindhe, 2005). Furthermore, if tooth loss has occurred due to chronic and/or acute infections, or severe periodontal disease or trauma, the resulting residual ridge will often be deficient and may cause difficulties in inserting an implant of adequate dimensions. To remedy such a situation where no optimal bone volume is available, several solutions have been proposed: i) tilted implants (Aparicio *et al.*, 2001; Chrcanovic *et al.*, 2015) ii) short implants (Neldam & Pinholt, 2012; Monje *et al.*, 2013) iii) bone augmentation procedures, either concomitant with implant placement or as staged interventions(McAllister & Haghighat, 2007; Chiapasco *et al.*, 2009; Esposito *et al.*, 2009; Benic & Hämmerle, 2014). The first and the second options aim to achieve an implant-supported fixed restoration when bone volume is poor, without bone augmentation procedures. The advantages include a reduction of costs, surgical time, healing time and morbidity of the patient. Bone augmentation procedures, on the other hand, offer a higher likelihood for oral implant rehabilitations in atrophic bone ridges, at the expense, however, of higher costs, longer surgical time and healing time, as well as increased morbidity. Many studies have shown that the survival rates of implants placed in augmented bone are comparable to survival rates of implants placed in native bone(Hämmerle & Jung, 2002; Chiapasco & Zaniboni, 2009; Jensen & Terheyden, 2009).

Biology of bone augmentation procedures

Bone tissue is a dynamic mineralized connective tissue (Kalfas, 2001). Anatomy, histology and biochemistry of this tissue have already been described in detail: an exhaustive description of these issues can be found in the recommended citation. The following paragraph will briefly describe the embryology of the bone, as it has many similar features to those that occur during bone regeneration.

At the time of its embryological development, bone formation follows two different pathways: i) endochondral ossification (EC) and ii) intramembranous ossification (IM) (Gilbert, 2000). EC happens through a replacement of a pre-existing cartilage matrix by bone. The mechanism of IM starts from mesenchymal tissue that directly differentiates in mineralized bone tissue (figure 1 and 2). It has been reported that only the latter is the mechanism involved in all intraoral bone augmentation techniques(McAllister & Haghighat, 2007). On the other hand, the healing process after bone fracture clearly presents both these modalities(Gerstenfeld & Cullinane, 2003; Dennis *et al.*, 2014). To this day, there are no other options to obtain new bone tissue formation than provoking a surgical wound in the target area and trying to drive the wound healing process trough an ossification pathway. It was furthermore proven that in bone fracture repair, the absence of inflammatory mediators has a negative influence on the bone healing (Cho *et al.*, 2001).

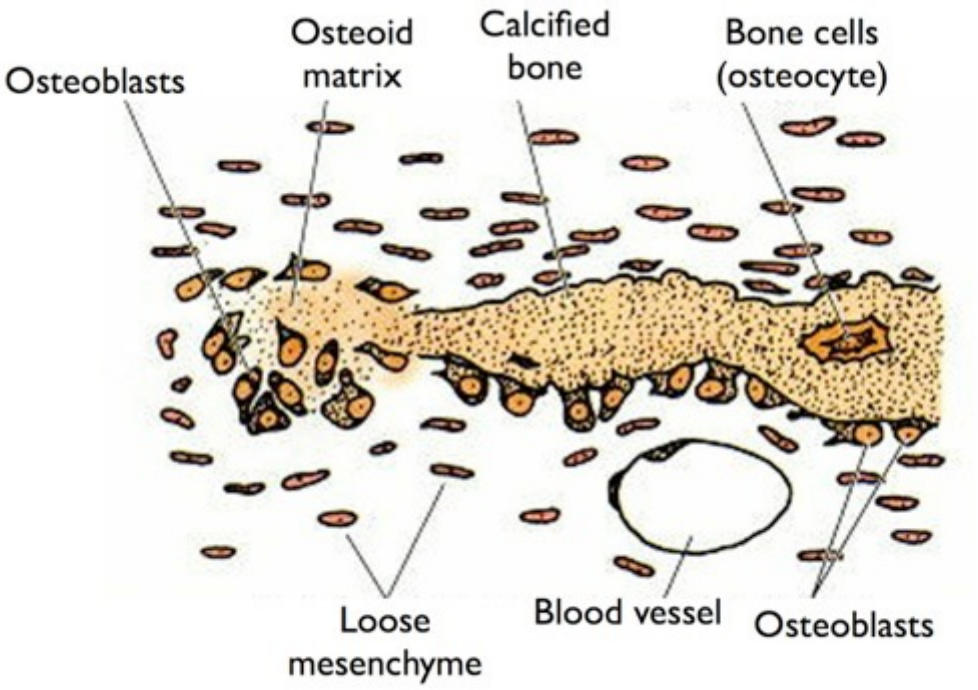

Figure 1 . 1 Schematic representation of intramembranous ossification. From left to right, mesenchymal cells differentiate in osteoblasts, which deposit osteoid matrix. These osteoblasts become arrayed along the calcified region of the matrix. Some cells remain in the mineralized matrix and become osteocytes. (Modified from Gilbert SF (2000). Osteogenesis: the development of bones, 6 edn.ed. Sinauer. Developmental Biology, Sunderland,MA).

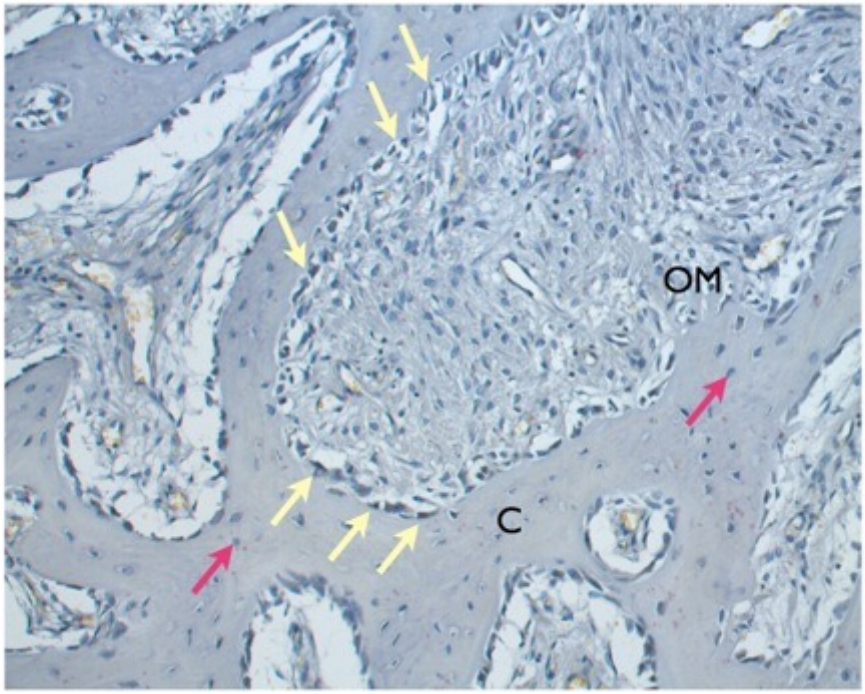

Figure 1 . 2 Intramembranous ossification occurred 2 weeks after bone augmentation procedure. Yellow arrows indicate arrayed osteoblast along the calcified region. Pink arrows indicate the osteocytes trapped in the bone matrix. C: calcified bone. OM: osteoid matrix. Toluidine blue stained, original magnification 200x.

Considering all these similarities, it could be assumed that bone augmentation surgery stimulates bone formation in a similar way that bone normally heals after an injury, i.e. with both EC and IM ossification pathways.

Bone augmentation techniques and applications

There are several bone augmentation surgical techniques described in the literature.

Growth factors (GF) have been extensively studied since researchers have believed for a long time that they are key factors in enhancing tissue regeneration(Kaigler *et al.*, 2006; Devescovi *et al.*, 2008). Above all GF, platelet derived growth factor (PDGF) and the bone morphogenetic proteins (BMPs) are the most investigated, with a large body of *in vitro* and *in vivo* animal studies. Despite all the

efforts, there is a lack of evidence-based clinical recommendations for the use of GF in bone regeneration(Nauth *et al.*, 2011).

Another bioengineering approach for bone augmentation procedures is by means of stem cells. Unfortunately, human trial on cell therapy for oral bone regeneration failed to demonstrate a clear advantage compared to other therapies (Meijer *et al.*, 2008; Kaigler *et al.*, 2015).

Bone splitting and distraction osteogenesis both demonstrated their ability to augment the bone volume of an atrophic alveolar ridge. On the other hand, both these procedures have some drawbacks and disadvantages that limits their use in favour of other approaches(Chiapasco *et al.*, 2009).

Bone grafting procedures and guided bone regeneration (GBR) sufficiently proved their clinical efficacy and predictability and will be described in a dedicated paragraph.

The following are normally considered the main applications of bone augmentation techniques in the oral cavity:

a) Alveolar ridge preservation following tooth extraction;
b) Alveolar ridge augmentation:
    a. in the horizontal dimension,
    b. in the vertical dimension (including sinus lift procedures);

For the purpose of this work, only atrophic ridge augmentation in the horizontal dimension by means of GBR will be further discussed in details.

Principles of guided bone regeneration

GBR is the most frequently used and well documented bone augmentation procedure in dentistry (Chiapasco *et al*., 1999; Simion *et al*., 2001) (Buser *et al*., 2002). The principle of this technique was first described in 1959 for spinal fusion surgery (HURLEY *et al*., 1959). After that, guided

tissue regeneration (GTR) was theorized by Melcher in 1976(Melcher, 1976) for the regeneration of periodontal tissues around teeth. Based on the same biological principles, GBR was introduced by Dahlin between 1989 and 1990(Dahlin *et al.*, 1988; 1989). The idea was to use a barrier membrane to mechanically seclude the soft tissues cells from repopulating the osseous defect, and thus to allow the osteogenic cells from the bony walls to replace the blood clot with new bone tissue. The histological results of Dahlin's studies confirmed the hypothesis, showing also that the amount of new bone formation was directly correlated with the volume created between the membrane and the bone surface. Indeed, one of the limitations of this surgical technique was the lack of the space maintenance effect of currently existing barrier membranes, which clearly limits the potential for the achievement of enough ridge augmentation for ideal implant placement. To overcome this limitation, different bone replacement grafts (mainly particulate autografts, allografts or xenografts) have been used as a scaffold in order to maintain the ridge anatomy. With several technical improvements, the general mechanism of the GBR was accepted and confirmed over the years, and this combination approach has demonstrated successful outcomes over the past two decades (Hämmerle & Jung, 2003; Tonetti *et al*., 2008). In 2006, Wang and Boyapati suggested four basic principles that a surgical technique should account for for predictable bone regeneration (Wang & Boyapati, 2006): i) soft tissue cell exclusion; ii) space maintenance iii) blood clot stability and iv) primary wound closure. Today, within a substantial agreement on the other aforementioned principles, it could be debated whether the seclusion of epithelial and connective tissue cells from the augmented area is still to be considered a key factor for bone regeneration. This assumption could be revisited considering the successfully result of various techniques tested in several studies whereby means of porous titanium meshes the reconstruction of an atrophic bone ridge is achieved(Rasia-dal Polo *et al.*, 2014).

Barrier membranes

A barrier membrane (BM) was first tested in the oral cavity for GTR by Nyman in 1982 (Nyman *et al.*, 1982). Different types of barrier membranes have been used for GBR and their specific composition falls into two broad categories: i) non-resorbable and ii) resorbable.

Non-resorbable membranes have been frequently used in bone regeneration obtaining the best results in terms of augmented bone volume(Tinti *et al.*, 1996). Non-resorbable membranes were mostly made with expanded-Polytetrafluoroethylene (e-PTFE, commercialy known as Gore-Tex®) a micro-porous plastic polymer. In order to provide enough space between the membrane and the atrophic jaw, tenting pins were fixed to the bone. A second generation of e-PTFE membranes were reinforced with titanium strips, thus providing the space-making requirements needed for bone regeneration. The main concern about the e-PFTE membrane was the low resistance to bacterial contamination due to its rough surface. A third generation of non-resorbable membrane partially reduced this problem by using a dense PTFE (d-PFTE) instead of an expanded one. The dense PTFE resulted in a smoother surface which shows better behaviour in the case of membrane exposure to the oral environment(Urban *et al.*, 2014; Ronda *et al.*, 2014).

The need of a second surgical intervention to remove these kind of membranes and the relatively high incidence of postoperative complications, mainly early membrane exposure, has limited their clinical use, thus resulting in the much broader use of biodegradable membranes.

Resorbable BM can be further divided in two categories: i) collagen and ii) polyglicoside syntetic copolymers. Geistlich Bio-gide® (Geistlich Biomaterials, CH-6110 Wolhusen, Switzerland) is a non cross-linked resorbable BM (figure 3). It comprises type I and III collagen of porcine origin. It has a bilayered structure; one side of the membrane is covered by densely packed collagen fibres designed to face the soft tissues, and the other side is rough allowing the osseoprogenitor cells to grow into the defect. Resorbable membranes based on synthetic polymer (e.g. polylactic acid) were the first approved by the American Food and Drug Administration for clinical use. Nowadays their use in clinical practice is limited.

Figure 1 . 3 Clinical aspect of a resorbable barrier membrane covering a particulate xenogeneic graft in an horizontal bone defect. The membrane was fixed with metal pins.

Grafting material

Graft materials are commonly classified for their osteogenic, osteoinductive or osteoconductive potential.

A bone graft harvested from the same individual is called fresh autogenous graft and is considered the only one that has all the three characteristics (although studies of graft cells viability have shown that very few of these transplanted cells survive). During the augmented site healing process, bone grafts, either in particulate or in block, are involved in process called “creeping substitution”. Reabsorption of old necrotic bone occurs simultaneously with the formation of new viable bone through an IM pathway (Kalfas, 2001).

Allografts come from individuals of the same species of the host. They are commonly considered as osteoinductive and osteoconductive grafts.

Syntetic grafts are termed alloplasts, and contribute to bone formation with their space-mantaining ability (i.e. only osteoconduction), as the xenografts. Geistlich Bio-Oss® Collagen (Geistlich

Biomaterials, CH-6110 Wolhusen, Switzerland) is a bone xenogeneic graft in block form (figure 4) composed of 90% of spongiosa granules of deproteinized bovine bone mineral (DBBM) and 10% of a purified porcine collagen (DBBM-C).

Both collagen membrane and DBBM have been tested for their safety and their use is widespread in clinical daily practice, with good clinical results (Schlegel *et al*., 1997; Hämmerle *et al*., 2007; Jung *et al*., 2013).

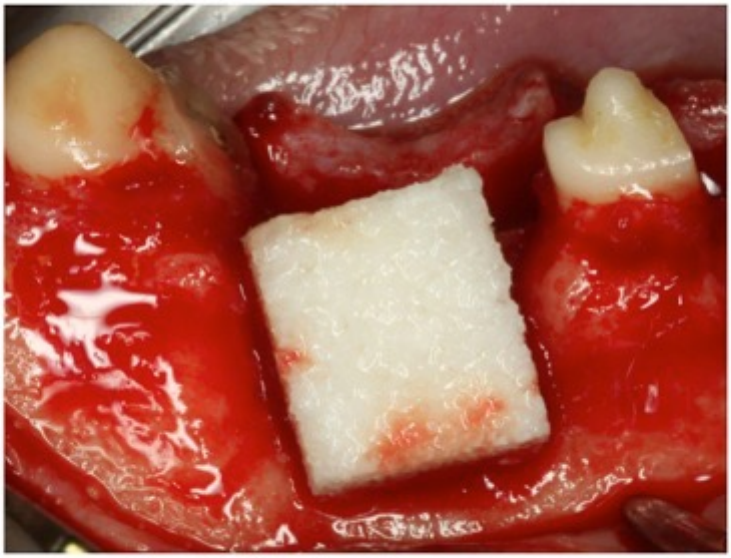

Figure 1 . 4 Clinical aspect of hydrated xenogeneic graft before shaping it and adapting it on the atrophic crest.

Horizontal bone defect

Depending on various local and/or systemic condition, a wide range of bone resorption can affect the edentolous alveolar processes of the jaws. The figure 5 shows a very well known classification published almost 30 years ago (Cawood & Howell, 1988) that is still one of the most cited in recent literature.

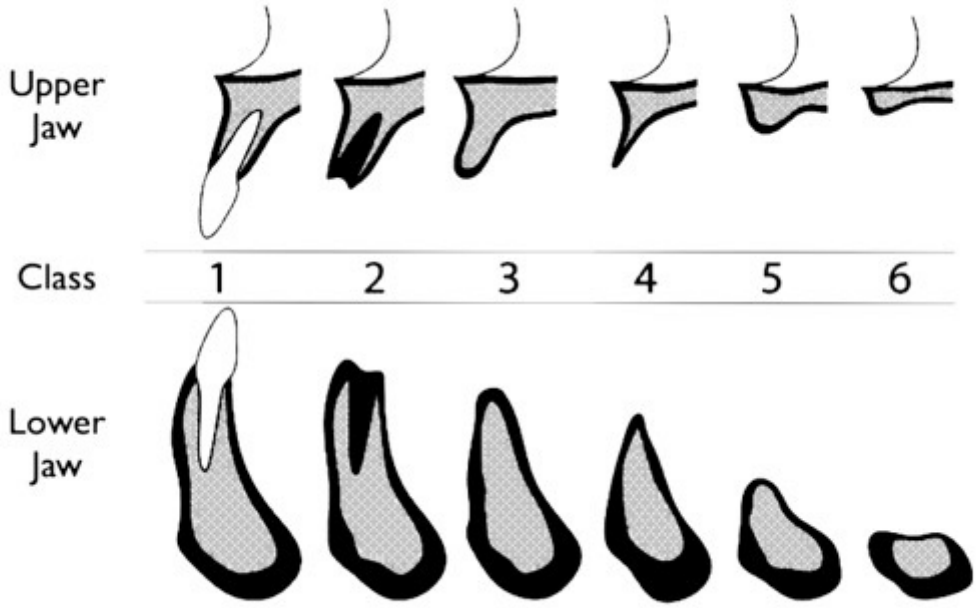

Figure 1 . 5 Cawood and Howell classification (1988). Class I: physiological condition with tooth. Class II: immediately after tooth extraction. Class III: presence of an adequate bone height and width. Class IV: knife-edge form with sufficient height and inadequate width of the alveolar process. Class V: flat ridge form with loss of almost all the alveolar process. Class VI: alveolar process totally reabsorbed and partial basal bone loss.

Cawood and Howell's classification is mainly based on adequate or inadequate bone height and width, and this could explain its wide use over the years. Since vertical bone augmentations are much more demanding and have a lower success rate, horizontal bone augmentations are more commonly used. Vertical bone augmentations for inadequate bone height has always been considered more challenging to solve than surgical approaches to remedy insufficient horizontal bone volume (Rocchietta *et al*., 2008). Complications such as membrane exposition happen more frequently in vertical bone augmentation procedures (Jensen & Terheyden, 2009). On the other hand, horizontal bone augmentation is considered a predictable technique for inadequate bone width, and GBR is a validated surgical approach either with simultaneous implant placement or in a staged procedure (Nevins *et al*., 1998; Donos *et al*., 2008; Benic & Hämmerle, 2014).

.

Aims of the study

The aims of this pre-clinical in vivo study are: a) to study the influence of the biomaterials used in GBR procedures (barrier membrane and xenograft bone replacement graft) when used either alone or in combination for the treatment of experimentally created chronic horizontal bone defects (class 4 of Cawood and Howell) in dogs; b) to analyse the variations in tissue composition at different time points (4 days, 2, 6 weeks and 3 months of healing) c) to investigate which factors may be correlated with the outcomes of the augmentation surgery.

Chapter two

Material and methods

This *in vivo* experimental investigation was designed as a prospective three arm, balanced block randomized, examiner-blind experimental study, evaluating four healing periods after the reconstructive procedure (4 days, 2 weeks, 6 weeks, 3 months).

Sample and facilities

The study protocol was approved by the Ethical Committee of the Rof Codina Foundation at the University of Santiago de Compostela (Spain). Eighteen female beagle dogs, with an age ranging between 1,5 and 2 years and a weight ranging between 10 and 20 kilograms, where used for this experiment. This experimental investigation was designed following the modified Arrive guidelines for pre-clinical research (Vignoletti & Abrahamsson, 2012). The procedures were performed according to Spanish and European Union regulations about care and use of research animals, in accordance with the European Communities Council Directive (86/609/EEC). All animals were fed on a soft pellet diet and maintained in individual kennels in a 12:12 light/dark cycle and 22-21 Cº as well as monitored daily during all the study phases by an experienced veterinarian in the animal experimentation service facility at the Veterinary Teaching Hospital Rof Codina of Lugo (Spain) during the year 2012.

Surgical procedures

All surgical procedures were carried out between June and December 2012. After animal sedation with propofol (2mg/kg/i.v., Propovet, Abbott Laboratories, Kent, UK), general anesthesia was mantained under mechanically induced respiration of 2,5-4% of isoflurane (Isoba-vet, Schering-Plough, Madrid, Spain). The animals were premedicated with acepromazine (0,05 mg/kg/i.m., Calmo Meosan, Pfeizer, Madrid, Spain), and morphine (0,3 mg/kg/i.m., Morfina Braun 2%, B. Braun Medical, Barcelona, Spain) was administered as analgesic medication. Lidocaine 2% with epinephrine 1:100000 (2% Xylocaine Dental, Dentsply, York, PA, USA) was infiltrated locally to reduce bleeding during surgery.

Surgery 1 - defect preparation

The experimental model used in this study is outlined in figure 2.1.

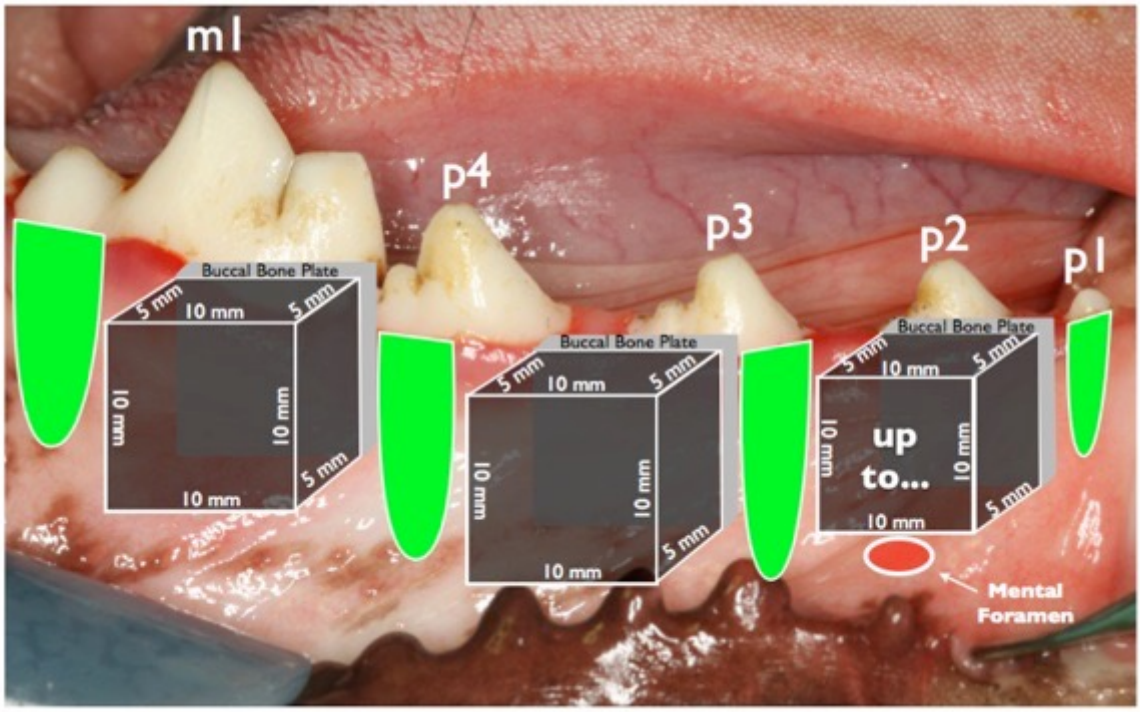

Figure 2 . 1 Schematic description of the experimental model. Three 10x10x5 mm defects (dark grey cube) were shaped between the remaining roots (green). The buccal bone plate (light grey square) was preserved.

On both sides of the mandible, the buccal and lingual mucoperiosteal flap was raised (figure 2.2). The second, third and fourth lower premolars (P) and the first molar (M) were hemisected by means of a Lindemann bur. The mesial root of M1, the mesial root of P4, the distal root of P3 and booth roots of P2 where extracted (figure 2.3 and 2.4). A pulpotomy with a sterile bur was made in the residual root. After the bleeding was controlled, a dental pulp cap was made with calcium hydroxide (Dycal, Dentsply, York, PA, USA). Between the remaining tooth remnants, three standardized defects (P2, P3-P4 and M1) were shaped on the buccal aspect of each hemi-mandible with diamonds bur under copious sterile saline irrigation (figure 2.5).

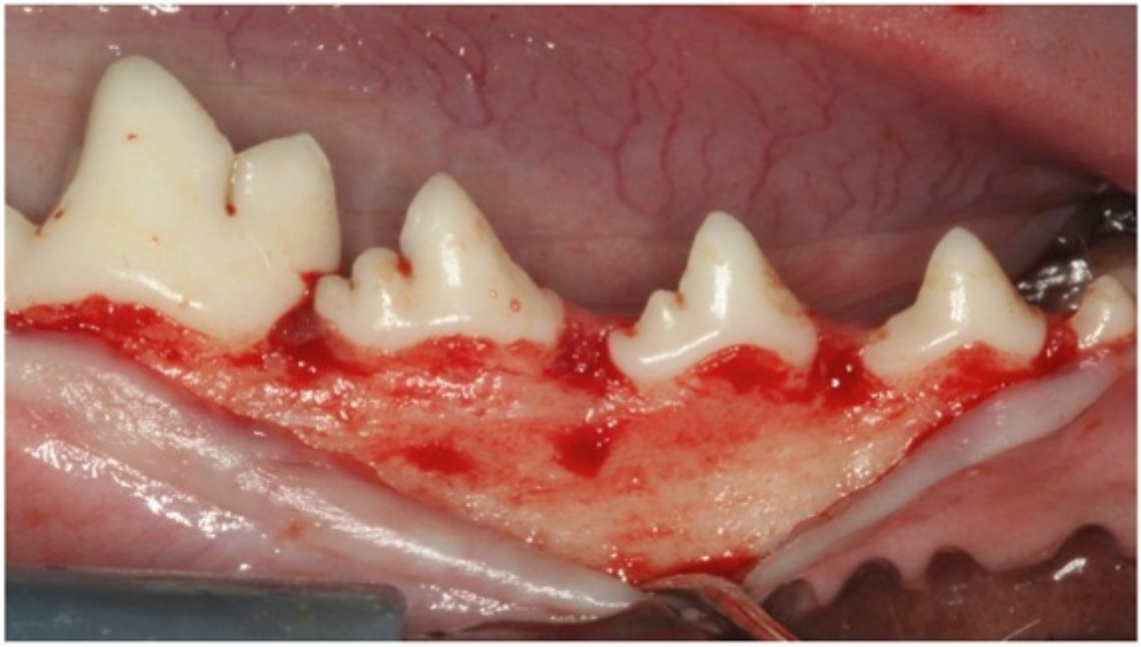

Figure 2 . 2 Surgery 1: full thickness flap elevation

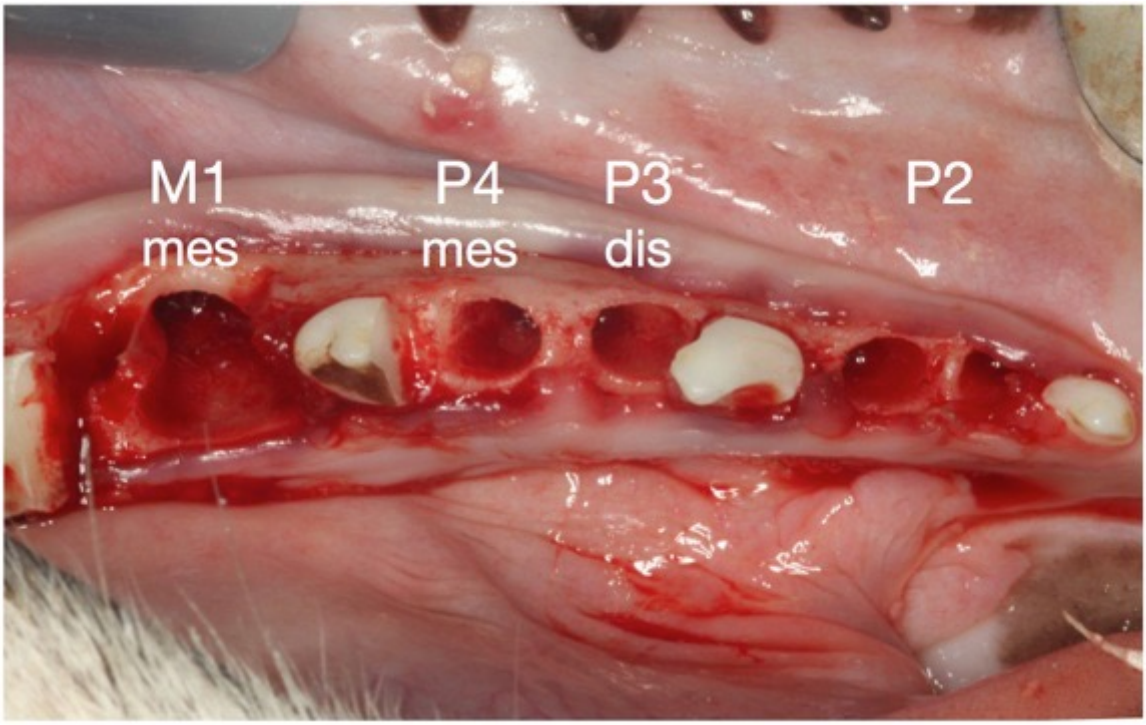

Figure 2 . 3 Teeth emisection and selective root extraction (mes=mesial; dis=distal).

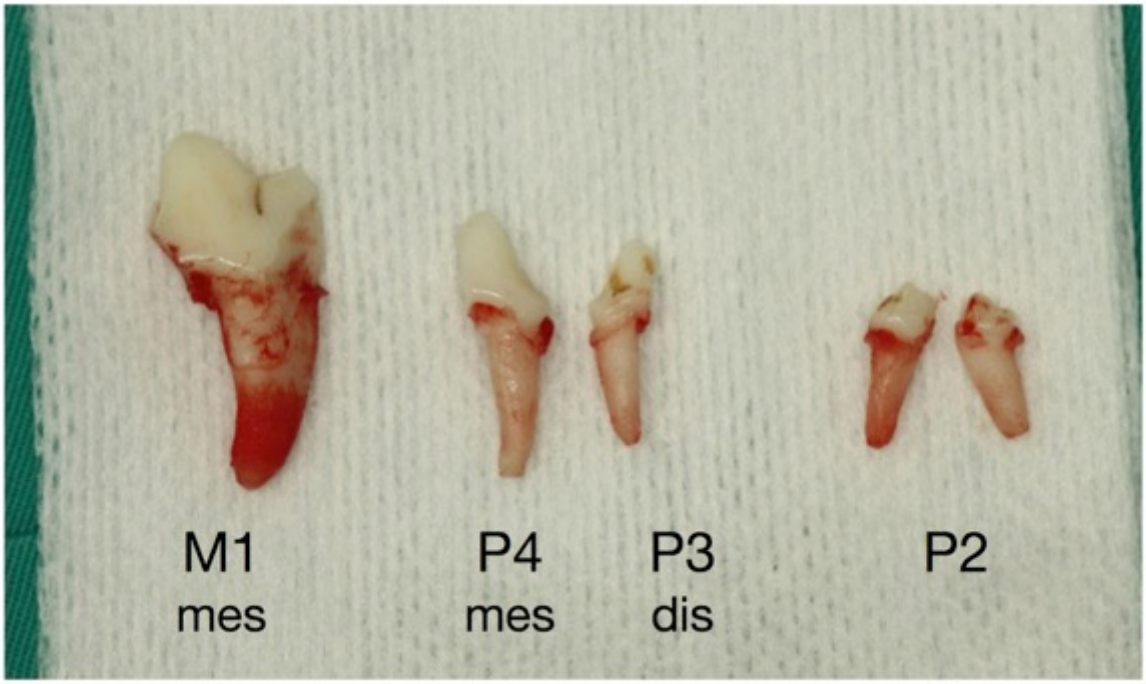

Figure 2 . 4 Extracted roots (mes = mesial; dis = distal)

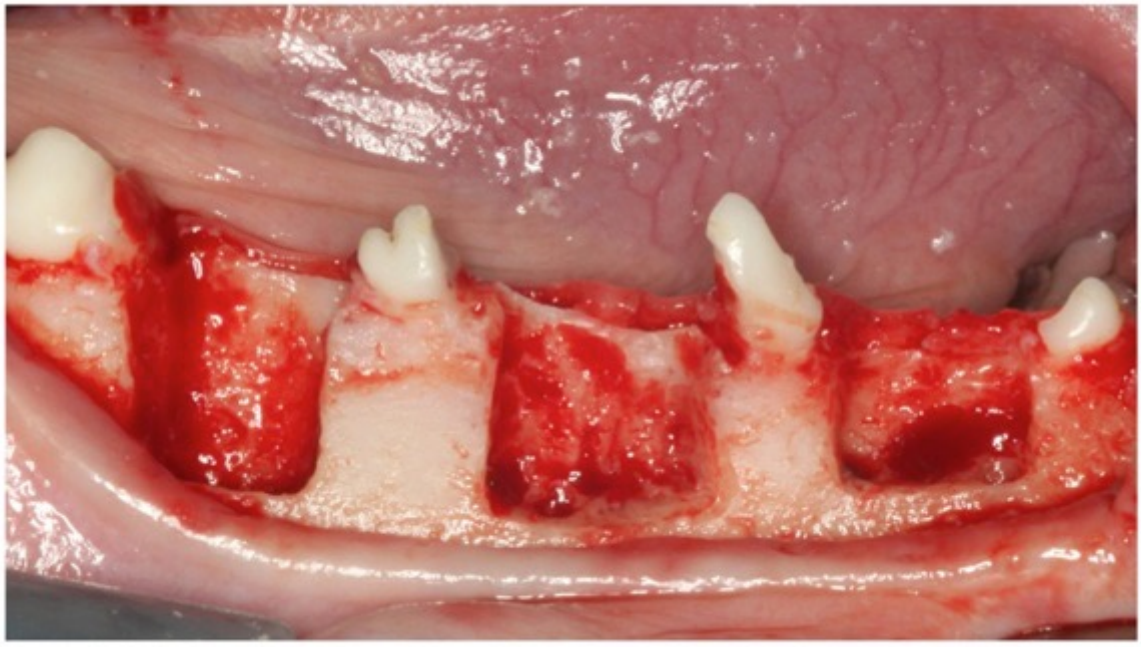

Figure 2 . 5 Bone defects shaping

Attempts were made to standardize the defect according to the following dimensions: 10 mm of vertical defect height from the most coronal lingual bone crest, 10 mm of mesio-distal defect width and 5 mm of bucco-lingual depth. At the end of the defect creation, the following clinical measurements were recorded for each defect:

- bucco-lingual horizontal width,
- mesio-distal horizontal width,
- apico-coronal vertical height.

A periodontal probe (PCP-UNC 15, Hu-friedy, Leimen, Germany) was used for clinical measurements. Flaps were finally repositioned and sutured with resorbable interrupted suture (Vicryl" 4.0, Johnson & Johnson, St-Stevens-Woluwe, Belgium).

Surgery 2 - augmentation procedure

After a healing period of minimum three months following the timeline of the study depicted in figure 2.6, the augmentation procedures were performed on both hemi-mandibles. The dogs were divided into two groups, A and B, providing two healing times per group (n=9). Briefly, a crestal incision was made in the edentulous areas and continued in the sulcus of the teeth from the distal aspect of the M1 to the mesial aspect of the P1. Full thickness buccal and palatal flaps were widely raised, isolating the mental nerve when necessary. Once exposed, the cortical bone was debrided with a sharp instrument to remove the residual connective tissue (figure 2.7).

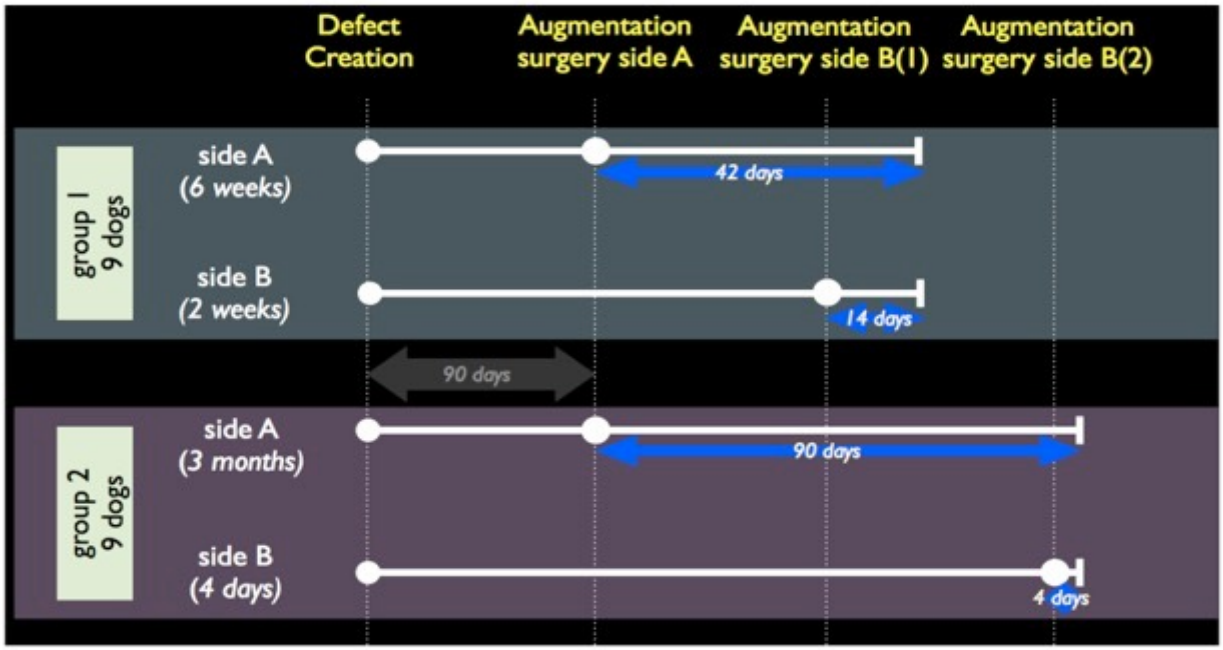

Figure 2 . 6 Timeline of the surgical phases of the study. The dark grey thick arrow indicates the defect chronification period. The blue thin arrows indicate the four different healing periods after the regeneration procedure. Side A and B can be either left or right emi-mandible, depending on the randomization.

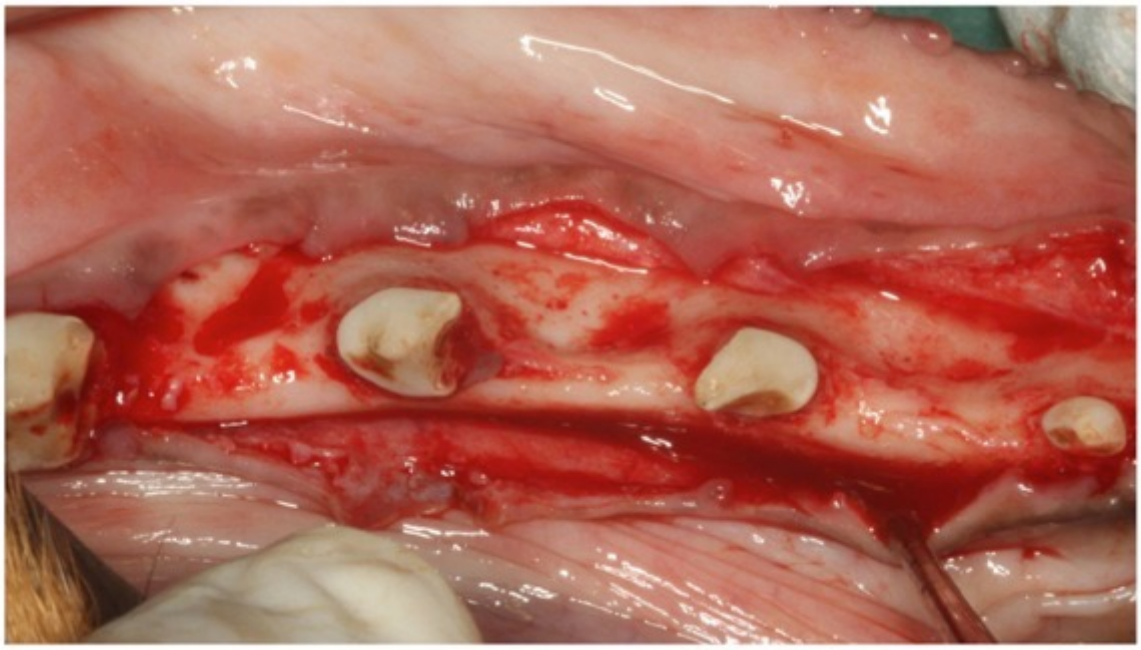

Figure 2 . 7 The chronic defects after 3 months healing period

Prior to treatment the following measurements of the each chronic defect were taken with a periodontal probe:

a) the bucco-lingual width of lingual bone plate
b) the horizontal bucco-lingual depth, defined as the distance between the lingual bone plate and a line parallel to the buccal bone of the adjacent teeth (figure 2.8).

Following cortical osteotomies preparation, a computer generated randomization list allocated each defect of one hemi-mandible to one of the three tested augmentation procedures (figure 2.9):

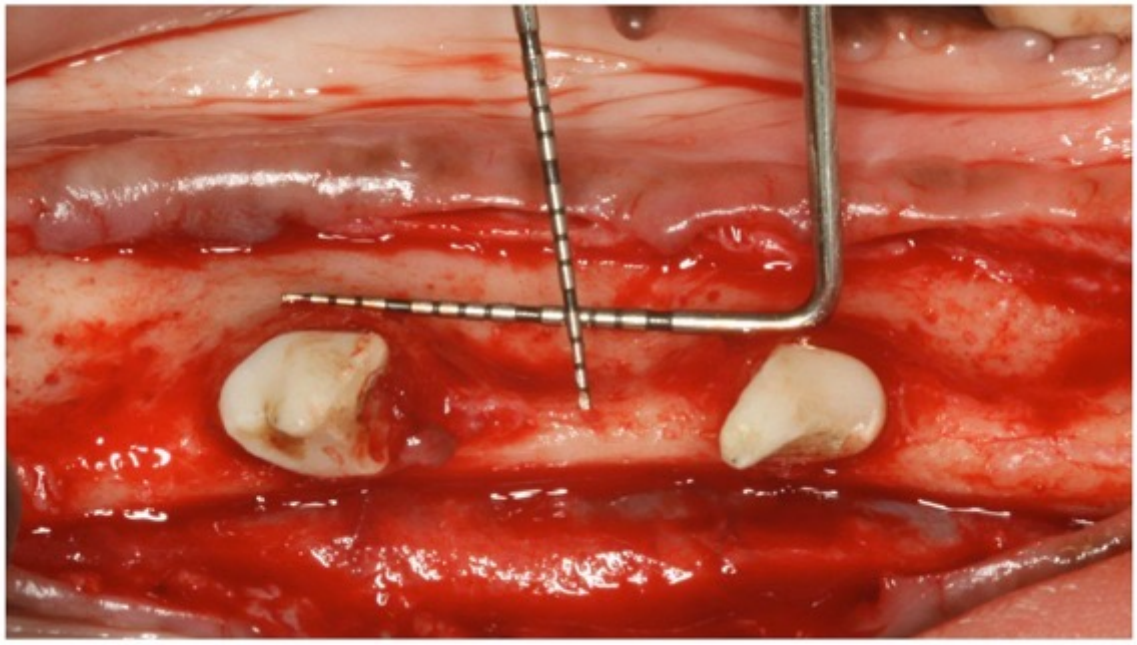

Figure 2 . 8 Measurement of the bucco-lingual depth of the chronic defect at the beginning of augmentation surgery.

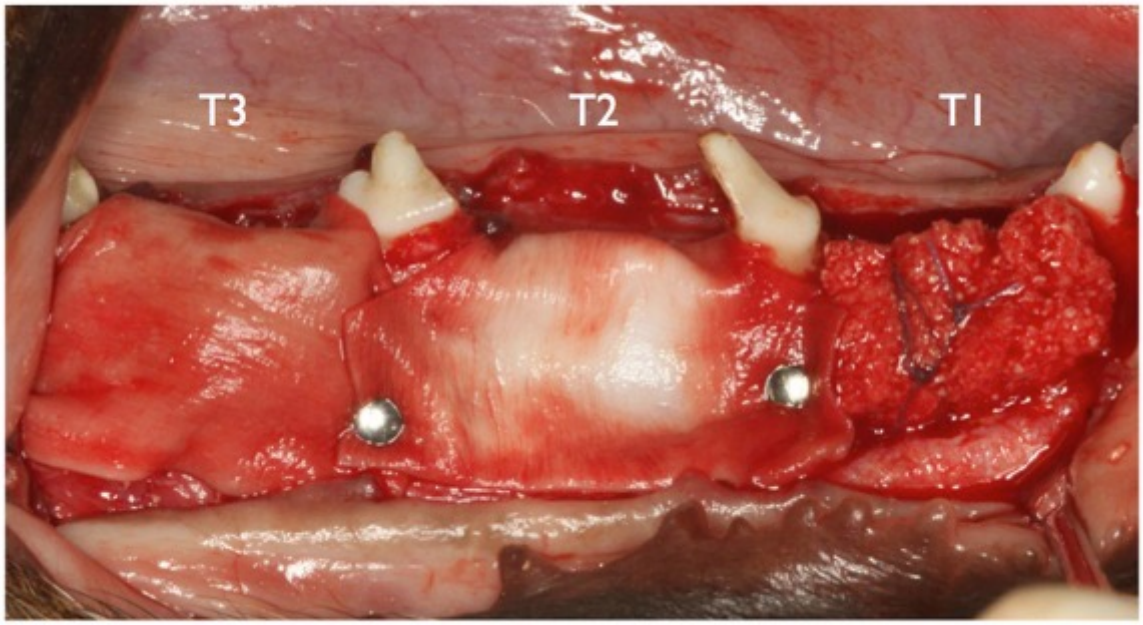

Figure 2 . 9 Augmentation treatment for each defect (T1 = graft only; T2 = membrane only; T3 = combined treatment).

1. T1. Xenogeneic Graft : the defect was filled with the DBBM-C. The xenograft was hydrated with saline and stabilized with a resorbable suture to the most apical portion of the buccal and the lingual periostium .
2. T2. Barrier membrane: the defect was covered with the BM. The membrane was trimmed and adapted over the ridge to completely cover the defect and extended beyond the defect margins by 2–3mm. The BM was secured in position by attaching four titanium pins (Frios membrane tacks, Dentsply, York, PA, USA) in the buccal and lingual bony walls.
3. T3. The combined treatment: the defect was filled with the DBBM-C and the BM was adapted to completely cover the defect and extended beyond the defect margins by 2–3mm.

The membrane was secured as previously described. Releasing incisions were made in the periosteum at the base of the buccal and lingual flaps and the augmented defects were carefully covered by tension-free flaps. Primary intention healing was achieved with horizontal internal mattress sutures alternated with interrupted 5/0 e-PTFE sutures (Goretex Suture, W. L. Gore & Associates Inc. Newark, DE, USA).

Postoperative care

Morphine (0,3 mg/kg/i.m.) was administered for the first 24 hours and meloxicam (0,1 mg/kg/s.i.d./p.o., Metacam, Boehringer Ingelheim España, Barcelona, Spain) for 3 days after surgeries to control pain. A 7 days post-operative antibiotic therapy was set with amoxicillin (22mg/kg/s.i.d./s.c., Amoxoil retard, Syva, León, Spain). During 14 days after surgeries, the animals were fed only with water-softened food instead of soft pellet to prevent rupture of the sutures and surgical wounds were cleaned three times a week using gauzes soaked in chlorexidine mouthrinse (0,12%). After 14 days sutures were removed.

Sacrifice and Histological processing

Dogs were sedated and than euthanized following the time table of the study (fig. 2.6) by an overdose of sodium pentobarbital (40-60 mg/kg/i.v., Dolethal, Vetoquinol, France). Each emi-mandible was removed and, before fixing it with buffered formalin, the caudal cortical bone of the jaw was separated from the biopsy to open the medullar spaces. The specimens were demineralized in EDTA, dehydrated using ascending grades of alcohol and embedded in paraffin. Every specimen was sectioned in a bucco-lingual plane trough the center (mesio-distally) of each critical defect. 5µm thick section were cut and stained with haematoxylin and eosin (HE) for histological examination.

Histometric and Histomorphometric assessment

Qualitative and quantitative histometric and histomorphometric analyses were made using a Leica DMRBE microscope equipped with a Leitz DMRD micro-photographic unit (Leica Microsystems GmbH, Wetzlar, Germany) connected to a digital camera and a computer. Every section was acquired at 50x magnification in a high quality image (approximately 70-100MB each). Every assessment was performed with the image analysis software Image Pro Premiere 9.1 (Media Cybernetic Inc, Rockville, Maryand) according to the standardized nomenclature in bone histo-morphometry (Dempster *et al*., 2013).

HE stained sections were analysed under polarized light to distinguish between parent bone and the newly formed bone (figure 2.10) allowing the selection and isolation of the region of interest (ROI) for the histomorphometrical analysis. Presence and position of biomaterial particles, as well as muscle fibres, oral epithelium, alveolar nerve and mental foramen were also considered beyond the boundaries of the ROI. A blind calibrated examiner (L.F.) performed the assessment twice. Intra-examiner reliability of measurement was calculated with Intraclass Correlation Coefficient (ICC).

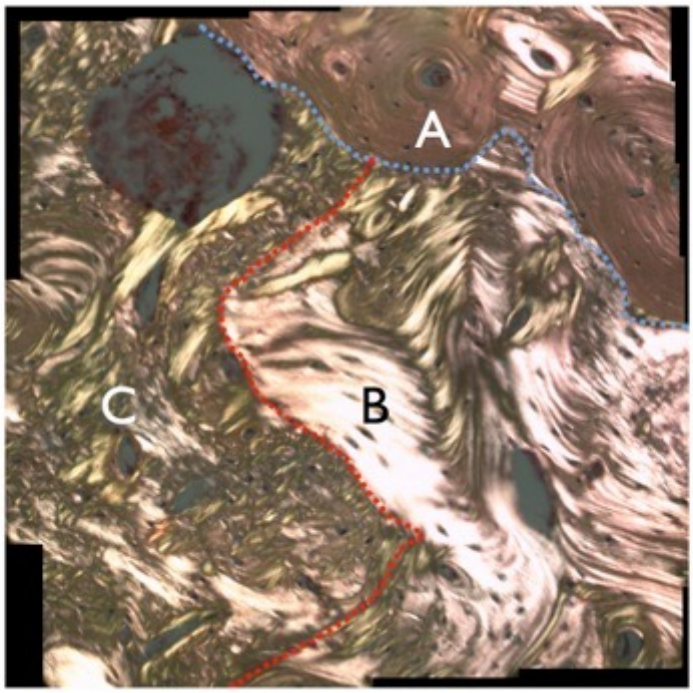

Figure 2 . 10 Microphotograph of mineralized tissue under polarized light. The blue line and the red line help to distinguish the three different stage of bone maturation: A. Mature bone. B. Lamellar bone formed after the surgery 1: (not included into the ROI area) C. Woven bone and lamellar bone formation after augmentation surgery (included into the ROI area). 3 months healing, polarized light. Hematoxylin-Eosin stained, original magnification 400x.

The shape of the ROI was analysed through two shape factors (dimensionless quantities that numerically describe the shape of a particle):

- Roundness (Ratio between major axis and minor axis of ellipse equivalent to region)
- Circularity (is defined as the degree to which an object is similar to a circle) (Olson, 2011)

Within the ROI, two-dimensional measurement were taken providing the following outcome measures:

- total area (mm^2) of augmented tissue (ROI)
- absolute (mm^2) and relative (% of ROI) value of bone replacement graft particles (DBBM-C)
- absolute (mm^2) and relative (% of ROI) value of mineralized structure
- absolute (mm^2) and relative (% of ROI) value of non-mineralized structure

An automated software feature called “smart segmentation tool”(SST) (figure 2.11) was used to calculate the area of each structure into the ROI, after validation of the software with manual counting. Using a differential method analysis of colour, shape, position, the SST could classify every pixel of the image and thus automatically recognize the several structures within the ROI. When an adequate level of discrimination between different structures was not achieved the SST result was judged to be unsatisfactory by the investigator and manual counting was performed.

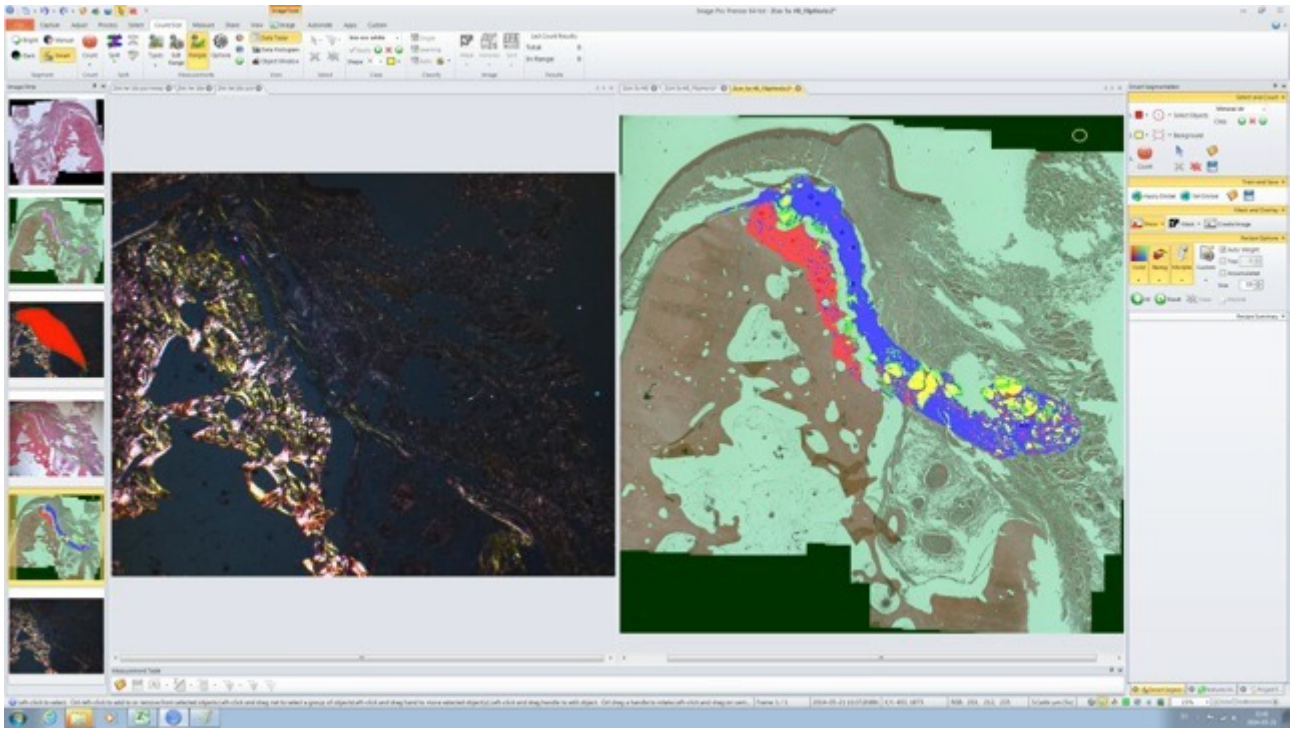

Figure 2 . 11 Image Pro Premiere graphic interface. The screenshot shows on the left an ematoxilin-eosin stained microphotograph under polarized light to distinguish between the different bone maturation types. On the right side, same image under non-polarized light with the ongoing smart segmentation tool feature.

Data Analysis

ICC were used to assess the intra-examiner reliability in ROI assessment.

Data from the histometric and morphometric evaluation were entered into an Excel (Microsoft Office 2011 for Mac) database and checked for entry errors. For each variable, mean and standard deviation were calculated. Clinical measurements of the chronic defects were tested for variance homogeneity (Barlett’s test), then either one-way ANOVA or Kruskal Wallis rank test was used for

inter-group comparisons and the Scheffe test for post-hoc estimation after ANOVA. Statistical analysis was performed with Stata11 (Stata/SE 11.0 for Mac. Stata corp).

Factors that may influence or were correlated with the histologic outcome variables of the bone augmentation procedure were analysed through a multivariate/multilevel model. A parsimonious model (namely, the "final model"), including the predictors that had a statistically significant impact ($p< 0.05$) on one or more dependent variables, was built. The coefficients were estimated using iterative generalized least squares (IGLS) and the significance of each covariate was tested using a Wald test. Nested models were tested for significant improvements in model fit by comparing the reduction in -2LL (-2 log likelihood) with a chi-squared distribution. A statistical package specifically designed for multilevel modelling was used (MLwiN 2.11r , Center for Multilevel Modelling, University of Bristol, Bristol, UK).

Statistically significant results were considered for p value < 0,05.

Results

Clinical findings

The post-operative healing was uneventful and the animals demonstrated good behaviour, as shown by their eating and drinking ad libitum.

The clinical results are depicted in Table 1. Defects at surgery 1 showed statistically significant differences among groups in terms of bone height, being M1> P3-P4 > P2. In surgery 2, these differences were statistically significant not only for bone height but also for bone crest thickness and defect depth, being M1>P2=P3-P4 and M1> P3-P4> P2, respectively. Since the treatment groups were randomised to the different defects, there were no differences when the different groups were compared at Baseline (Kruskal Wallis test, p>0,05).

	Surgery 1 - defect creation			**Surgery 2 -** Treatment	
	Apico-coronal	**Mesio-distal**	**Bucco-lingual**	**Crest width B-L**	**Defect depth B-L**
Defect site					
P2	7,91 (1,07)*	9,61 (0,67)	3,76 (0,49)	2,03 (0,48)*	2,85 (0,62)*
P3 - P4	9,24 (0,84)*	10,88 (0,86)	4,53 (0,38)	2 (0,35)*	3,44 (0,54)*
M1	9,91 (0,60)*	10,79 (0,90)	5,92 (0,48)	2,85 (0,63)*	4,06 (1,02)*

* Inter-group statistically significant difference (K-wallis rank test, p<0,05)

Table 1 - Defect measurement at surgery 1 and 2. Mean values (SD) are in mm. Apico-coronal: vertical measurement of the defect height from the bottom of the defect to the most coronal lingual bone crest. Mesio-distal: horizontal measurement of the defect width between its mesial and distal bone limits. Bucco-lingual: horizontal measurement of the defect depth from its buccal limit to the lingual bone plate. Crest width B-L: the bucco-lingual width of lingual bone plate adjacent to the chronic defect. Defect depth B-L: the horizontal bucco-lingual width of the chronic defect, defined as the distance between the lingual bone plate and a line parallel to the buccal bone of the neighbouring teeth. P2: mesial defect in the P2 mesial and distal

position. P3-P4: central defect in the P3 distal root and P4 mesial root position. M1: distal defect in the M1 mesial root position

Histological Observations

4 days-healing (figure 3.1) – The atrophic bone ridges presented variable bucco-lingual dimension in agreement with clinical data collected during the augmentation procedure. Poorly represented soft tissues appeared detached from the underlying bone crest. In T1 group, the graft particles were trapped in a mature blood clot (figure 3.2) and rarely detectable (3 out of 9 specimens). In T2, the barrier membrane was rarely depicted (3 out of 9 specimens) either in direct contact with the bone crest or separated by a void occupied by a layer of blood clot. In T3, the histological picture was characterized by the scarce presence of graft granules (2 specimens). The barrier membrane was also rarely depicted (2 specimens) and detached from the underlying bone crest.

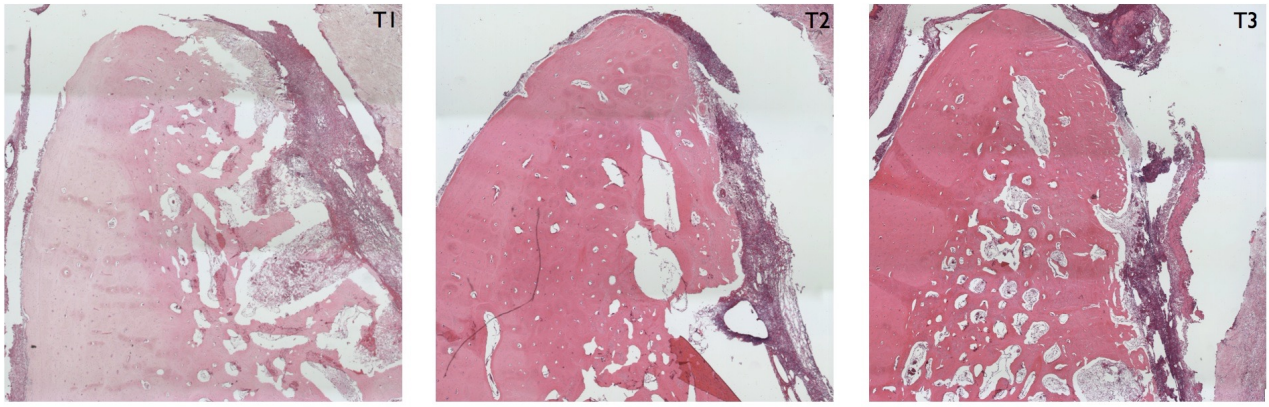

Figure 3 . 1 Histological samples of 4 days healing. T1 = only DBBM-C treatment; T2 = only BM treatment; T3 = DBBM-C + BM treatment. Hematoxylin-Eosin stained, original magnification 50x.

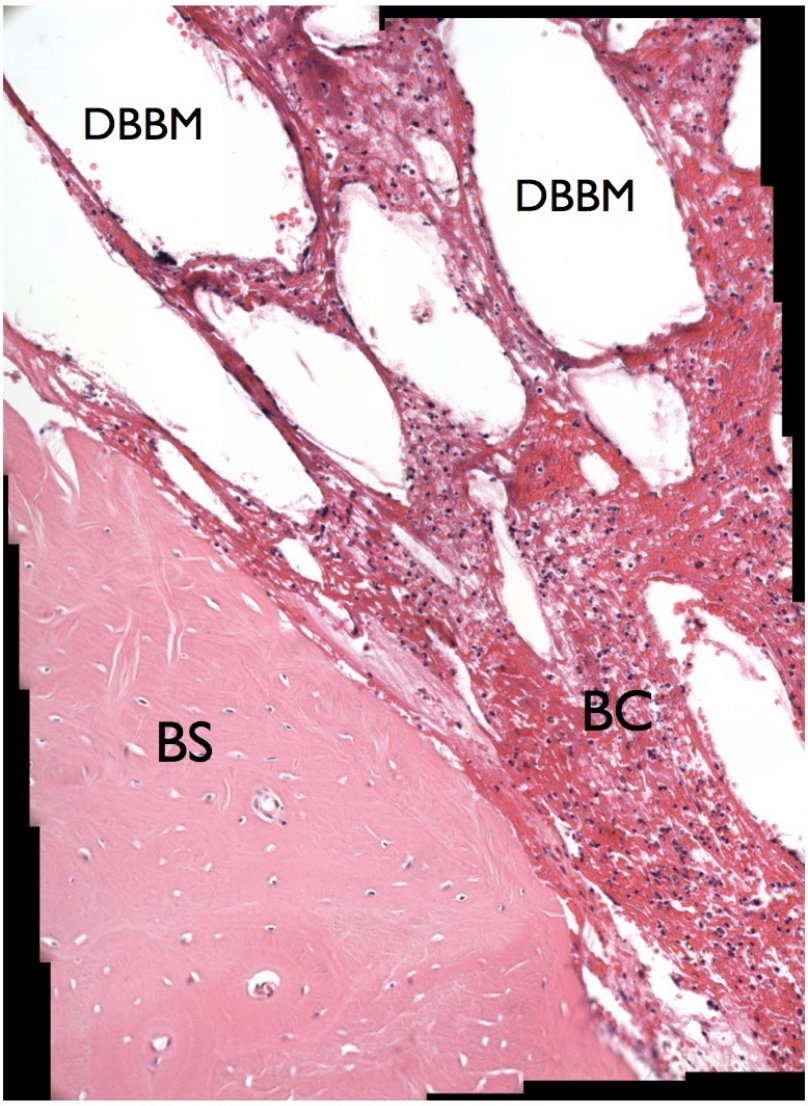

Figure 3 . 2 DBBM particle surrounded by blood (BC) clot in a 4 days section. BS: Bone surface. Hematoxylin-Eosin, original magnification 400x.

2 weeks healing (figure 3.3) – The augmented areas occupied a variable proportion of the ridge profile. Most of the tissue within the region of interest was represented by non-mineralized tissue and variable amounts of bovine bone graft particles. Occasionally, small areas of woven bone occupied the ROI, mainly close to its boundaries with the parent bone. No major differences were observed among the three groups. The graft particles were almost always surrounded by non-mineralized tissue and often densely accumulated in the apical portion of the ROI (figure 3.4). The collagen membrane was sometimes detectable although it appeared integrated within the host connective tissue (figure 3.5).

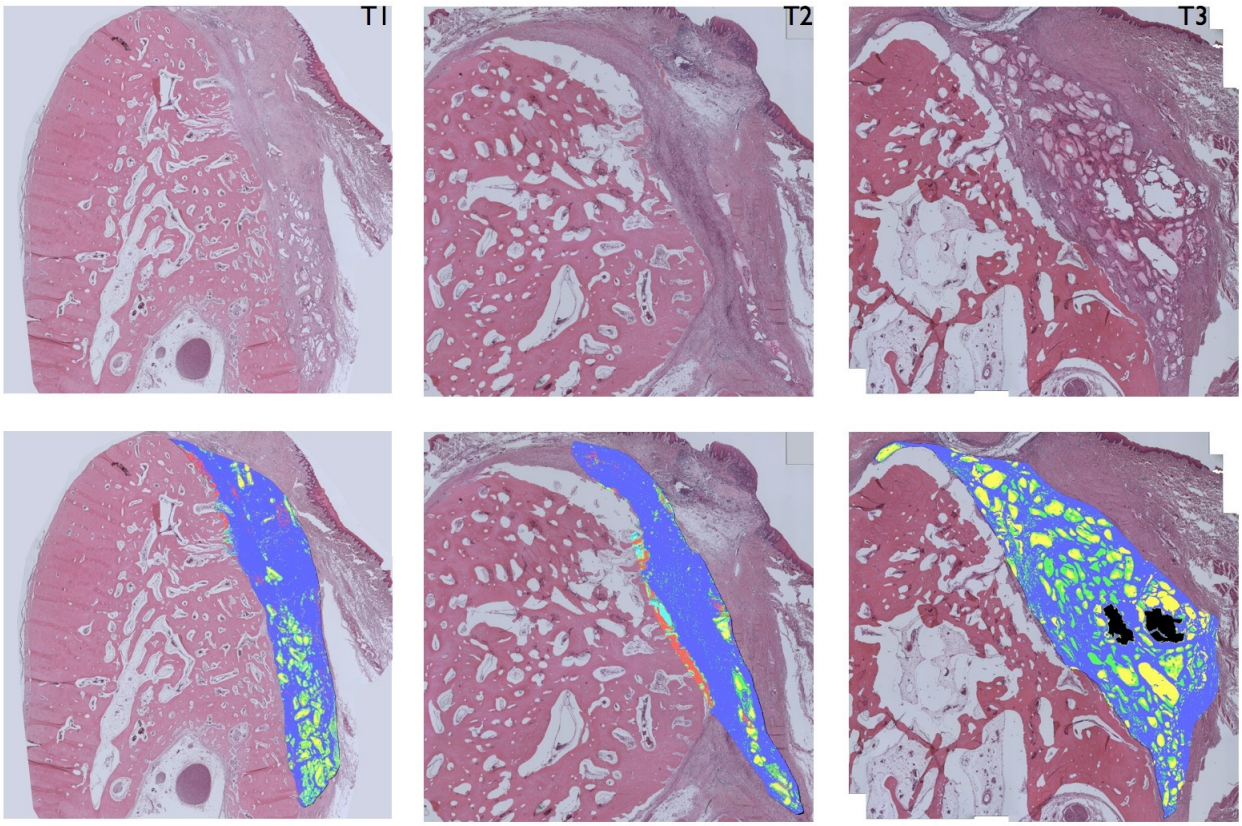

Figure 3 . 3 Histological samples of 2 weeks healing. T1 = only DBBM-C treatment; T2 = only BM treatment; T3 = DBBM-C + BM treatment. The colored area represents the Region of Interest (ROI) of the augmentation processes. Different colors represent different structures: dark blue = non mineralized structures; red = mineralized structures; yellow and green = deproteinized bovine bone mineral ; pale blue = medullar spaces. Hematoxylin-eosin stained, original magnification 50x.

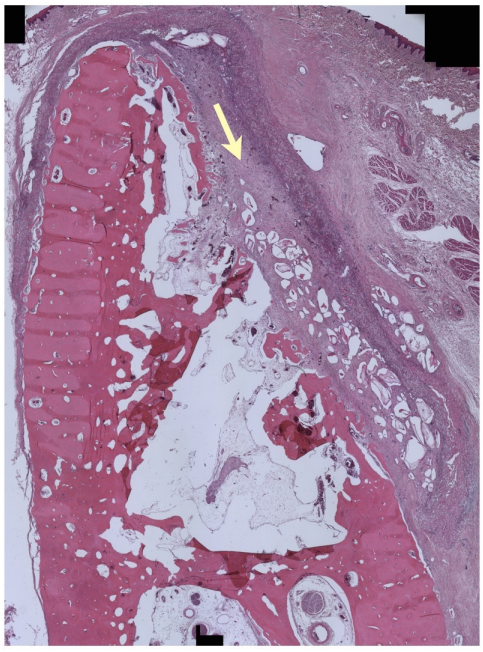

Figure 3 . 4 The DBBM particles are clearly displaced in a apical position (arrow). 2 weeks healing. Hematoxylin-Eosin stained, original magnification 50x.

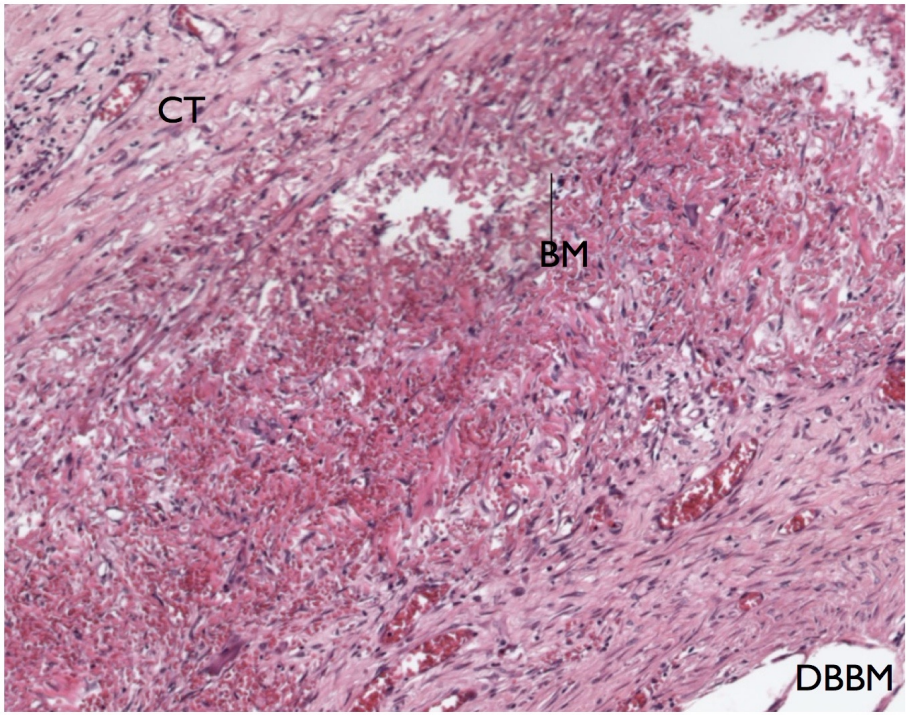

Figure 3 . 5 Particle of the section depicted in the figure 3.4. Barrier Membrane (BM) integrated in the host connective tissue. A DBBM particle is visible in the bottom right angle. CT: host connective tissue. 2 weeks healing. Hematoxyilin Eosin stained, original magnification 200x.

6 weeks healing (figure 3.6) – This healing period was characterized by the manifest presence of newly formed bone clearly visible in all treatment groups. A large number of different size graft particles were separated from the woven bone by a layer of variable thickness of provisional matrix of connective tissue in T2 and T3, whereas only occasionally the bovine bone particles appeared in contact with the newly formed bone. On the surface of some particles, multinucleated cells were present (figure 3.7). In T1 and T3 the structure of the barrier membrane couldn't be detected anymore except for some areas where traces of the bovine collagen graft were still observable.

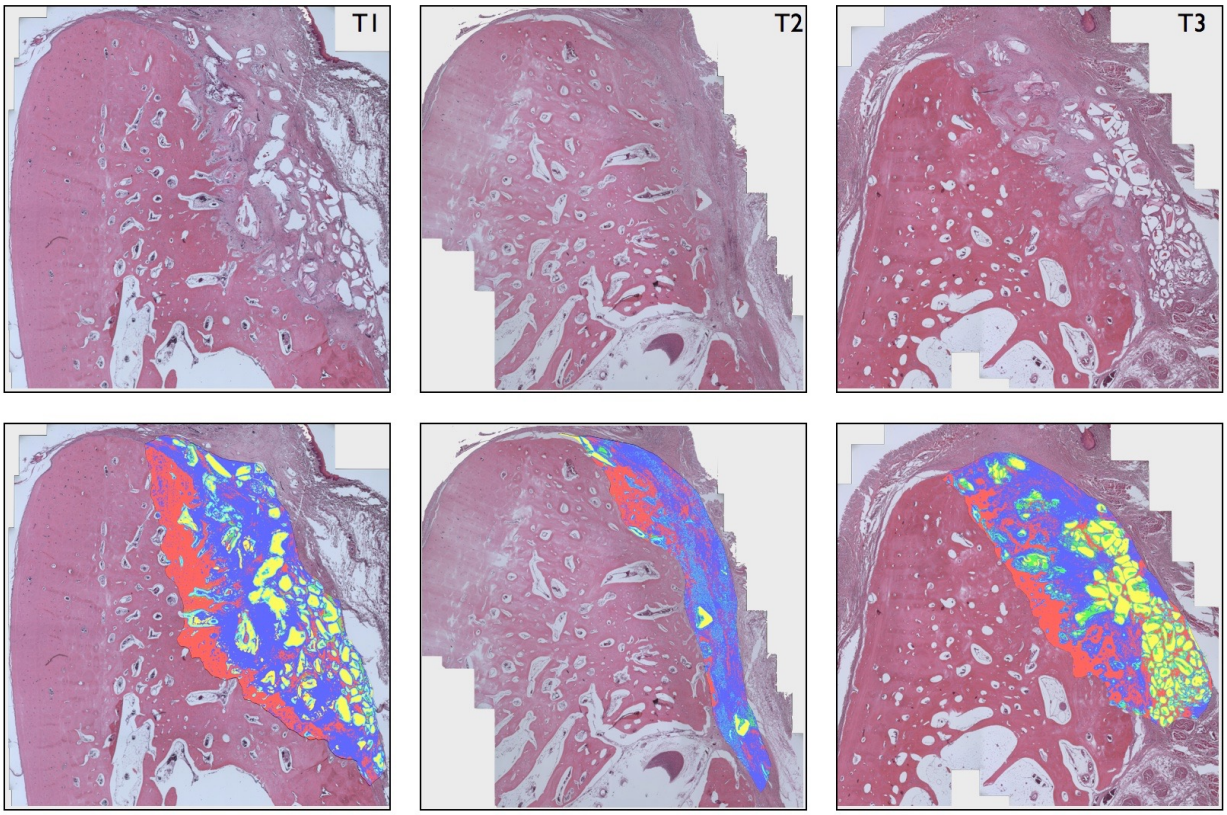

Figure 3 . 6 Figure 8 – Histological samples of 6 weeks of healing. T1 = only DBBM-C treatment; T2 = only BM treatment; T3 = DBBM-C + BM treatment. The colored area represents the Region of Interest (ROI) of the augmentation processes. Different colors represent different structures: dark blue = non mineralized structures; red = mineralized structures; yellow and green = deproteinized bovine bone mineral ; pale blue = medullar spaces. Hematoxyilin-eosin stained, original magnification 50x.

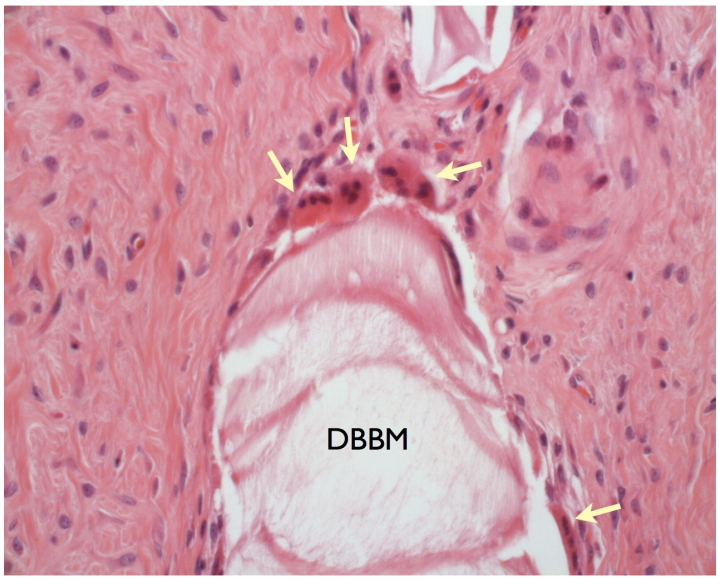

Figure 3 . 7 Figure 9 - DBBM particle surrounded by multinucleated cells (arrows). Hematoxylin-Eosin stained, riginal magnification 400x.

3 months healing (figure 3.8) – The woven bone has been remodelled and replaced mainly by lamellar bone that surrounded new medullar spaces (figure 3.9). A reduced number of graft particles of different sizes were detectable in both T1 and T3, being either in direct contact with the new lamellar bone or encapsulated within connective tissue. The barrier membrane was no longer detectable at this time.

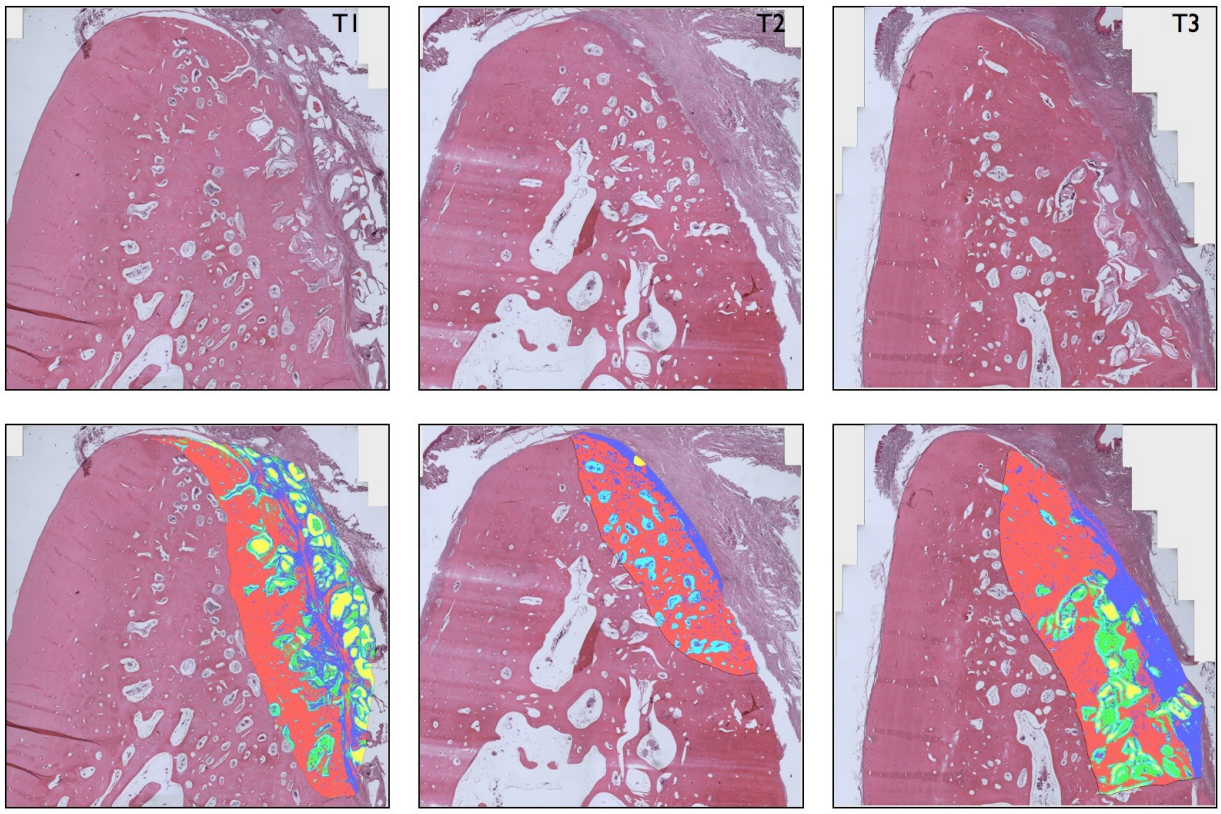

Figure 3 . 8 Histological samples of 3 months of healing. T1 = only DBBM-C treatment; T2 = only BM treatment; T3 = DBBM-C + BM treatment. The colored area represents the Region of Interest (ROI) of the augmentation processes. Different colors represent different structures: dark blue = non mineralized structures; red = mineralized structures; yellow and green = deproteinized bovine bone mineral ; pale blue = medullar spaces. Hematoxylin-eosin stained, original magnification 50x.

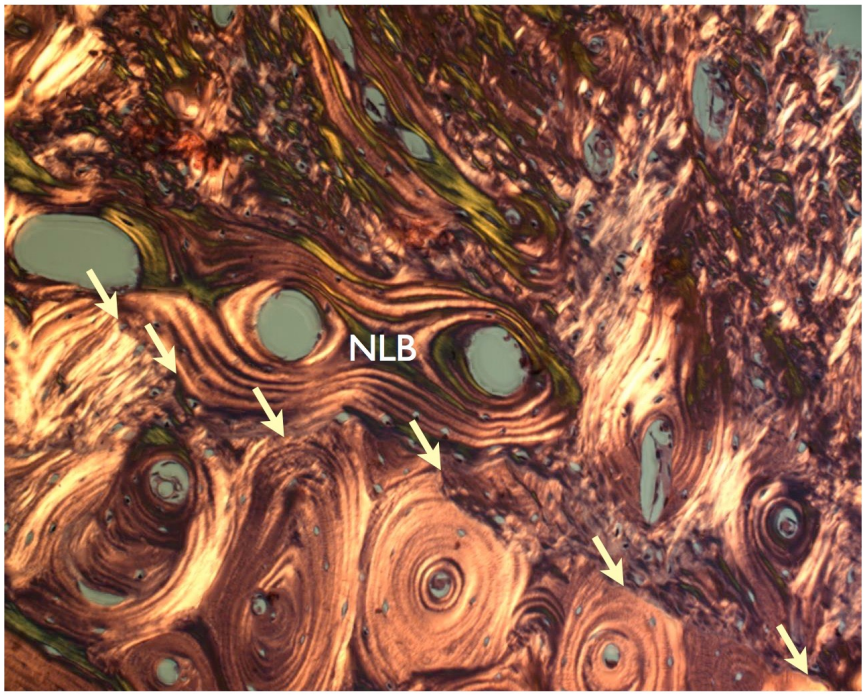

Figure 3 . 9 - Newly formed lamellar bone (NLB) into the ROI area. The arrows indicate the defect border. 3 months healing, polarized light. Hematoxylin-Eosin stained, original magnification 400x.

Histomorphometric results

The ICC score for intra-examiner reliability for ROI assessment was = 0,87 (high level of agreement).

Histomorphometric measurements were not performed in the 4 days specimens due to the early healing time interval.

Results of the histomorphometric measurements are presented in table 2 and figure 3.9. Table 3 presents the results of the multivariate/multilevel model. The explanatory variables included into the model are depicted in table 4.

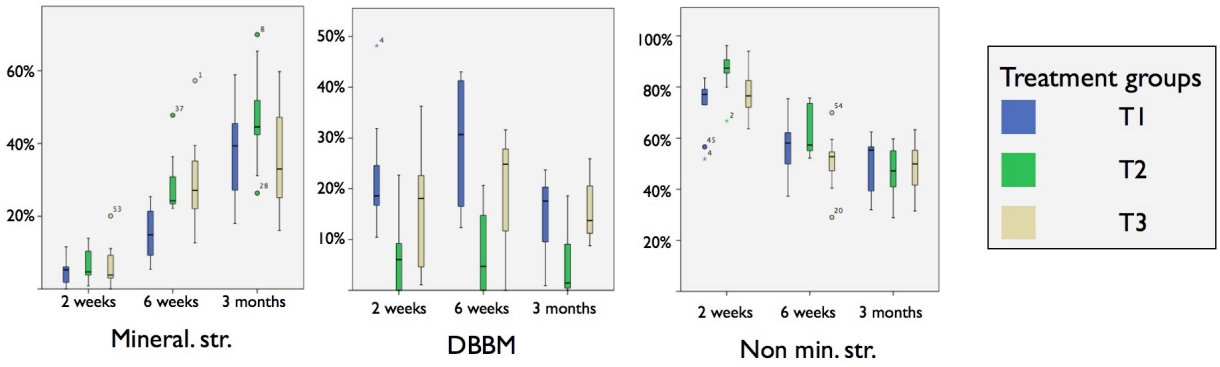

Figure 3 . 10 - Graphics of percentage of mineral structure (left), deproteinized bovine bone mineral (centre) and non mineral structure (right), divided for healing period and treatment.

Total regenerated area. A clear trend towards greater regenerated areas was observed for each treatment group and at each time interval being T3 > T1 > T2. Non-statistically significant greater ROIs were found at 6 weeks of healing (table 2). Statistically significant differences among the treatment groups were found in the multilevel regression analysis: the model revealed a statistically significant greater area in the T3 treatment group. A significant correlation between the bucco-lingual horizontal width of the defect and the total augmented area was observed: the deeper the defect, the greater the ROI. Furthermore, both shape factors showed a significant correlation between the shape of the ROI and its area: the greater the ROI, the more that ROI's shape resembled a circle.

	T1		T2		T3	
	mm^2	%	mm^2	%	mm^2	%
Two weeks healing						
Total ROI	9,83 (3,08)	100	7,28 (2,6)	100	9,88 (3,48)	100
DBBM	2,27 (1,26)*º	22	0,51 (0,72)*º	6	1,88 (1,65)º	17
Mineralized structure	0,49 (0,43)	5	0,39 (0,29)	6	0,57 (0,41)	7
Non-mineral. structure	7,07 (2,32)	73	6,38 (2,08)	88	7,43 (2,39)	76
Six weeks healing						
Total ROI	13,4 (9,2)	100	9,99 (4,92)	100	17,1 (8,68)	100
DBBM	3,79 (2,17)	29	1,03 (1,42)	7	4,19 (2,92)	22
Mineralized structure	2,4 (2,22)	15	3,23 (1,86)	33	4,21 (2,3)	26
Non-mineral. structure	7,23 (4,46)	56	5,73 (2,61)	60	8,67 (4,68)	52
3 months healing						
Total ROI	10,3 (4,01)	100	9,76 (3,89)	100	11,6 (4,87)	100
DBBM	1,46 (1,02)	15	0,73 (0,94)	6	1,76 (0,8)	16
Mineralized structure	4,04 (2,81)	37	4,46 (2,06)	47	4,23 (2,26)	36
Non-mineral. structure	4,78 (1, 55)	48	4,56 (2,21)	47	5,63 (2,92)	48

* Anova inter-group statistically significant difference (one-way Anova p<0,05)
º Post-hoc statistically significant difference (Scheffe's Test p<0,05)

Table 2 - Histological area assessment. Absolute values are described as mean (SD) in mm2; relative values are expressed as percentages (%) of the region of interest (ROI). Total ROI: the entire augmented area. DBBM: deproteinized bovine bone mineral. T1: only DBBM with collagen (DBBM-C) treatment group. T2: only barrier membrane (BM) treatment group. T3: combined (DBBM-C + BM) treatment group.

	Empty model	Standard error	Final model	Standard error	Sig.
Fixed Part: Total ROI (mm^2)					
Intercept	10,94	0,74	5,20	1,96	
Defect depth B-L (reference: 1 mm)			1,50	0,50	p<0,01
Treatment group (reference: T1)					
T2 treatment group			-0,33	1,00	p=0,74
T3 treatment group			2,04	0,96	p<0,05
Roundness (reference: grand mean)			-0,43	0,16	p<0,01
Circularity (reference: grand mean)			31,34	6,41	p<0,01
Fixed Part: % min tissue					
Intercept	0,2	0,0	-	0,0	
Crest width B-L (reference: 1 mm)			0,03	0,01	p<0,05
Defect depth B-L (reference: 2 mm)			0,04	0,01	p<0,001
Healing time (reference: 2 weeks)					
6 weeks healing time			0,18	0,02	p<0,001
3 months healing time			0,32	0,02	p<0,001
Treatment group (reference: T1)					
T2 treatment group			0,07	0,03	p<0,01
T3 treatment group			0,04	0,02	p=0,08
T2-T1 proximity (reference: no)			0,10	0,00	p<0,01
Roundness (reference: grand mean)			-0,01	0,00	p<0,01
Fixed Part: % DBBM					
Intercept	0,16	0,01	0,22	0,02	
Treatment group (reference: T1)					
T2 treatment group			-0,15	0,03	p<0,001
T3 treatment group			-0,04	0,03	p=0,055
Circularity (reference: grand mean)			0,30	0,11	p<0,01

Random part: Animal (n=18)					**Corr.**
Variance % DBBM	0	0	0	0	
Covariance % DBBM / % min tissue	0	0	0	0	
Variance % min tissue	0,01	0,01	0	0	
Covariance Total ROI / % DBBM	0	0	0	0	
Covariance Total ROI / % min tissue	-0,02	0,09	0	0	
Variance Total ROI	3,01	3,10	5,31	2,73	
Random part: Site (n=81)					
Varariance % DBBM	0,01	0,00	0,01	0,00	
Covariance % DBBM / % min tissue	-0,01	0,00	0,00	0,00	-0,48
Variance % min tissue	0,02	0,00	0,01	0,00	
Covariance Total ROI / % DBBM	0,24	0,08	0,09	0,04	0,27
Covariance Total ROI / % min tissue	0,15	0,10	-0,03	0,04	-0,10
Variance Total ROI	29,99	5,24	12,32	2,19	
-2 log likelihood	293,96		108,34		

Table 3 - Multivariate multilevel regression model on percentage of mineralized tissue (% min tis), percentage of deproteinized bovine bone mineral (% DBBM), and the entire augmented area (total ROI – region of interest) measured in mm2. Crest width B-L: the horizontal bucco-lingual width of the lingual bone crest. Defect depth: the horizontal bucco-lingual width of the chronic defect, defined as the distance between the lingual bone plate and a line parallel to the buccal bone of the neighbouring teeth. Treatment groups: T1 (only DBBM-C), T2: only barrier membrane (BM), T3: combined (DBBM-C + RM). T2-T1 proximity: all T2 sites that are not adjacent to a T1 site (see figure 3.10 for explanation).

Indipendent Variables	Categories	Min	Max
Crest width B-L		1 mm	4 mm
Defect depth B-L		2 mm	7 mm
Healing time	2 weeks / 6 weeks / 3 months		
Treatment groups	DBBM (T1) / BM (T2) / Combined (T3)		
T2-T1 proximity	Y / N		
Circularity		0,03	0,43
Roundness		1,75	20,74

Table 4 - Predictors tested in the model.

New bone formation. Similar areas of newly formed bone were observed at 2 weeks and 3 months among the groups, whereas at 6 weeks, almost twice the area of newly formed bone was observed in the T3 group as compared to T1, being T3 > T2 > T1. When these areas were calculated as proportions of the augmented region of interest this tendency changed. Indeed, the areas of new bone formation at 6 weeks of healing represented 33%, 26% and 15% of the region of interest in T2, T3 and T1, respectively. Regression analysis confirms that the T2 treatment group was statistically correlated with a higher proportion of mineralized tissue into the ROI. Furthermore, the proportions of newly formed bone increased significantly throughout the entire study period (12 weeks>6 weeks>2 weeks). A significantly higher percentage of mineralized tissue is also correlated with: i) the increase of the bucco-lingual width of the lingual bone plate; ii) the increase of bucco-lingual horizontal depth of the defect iii) the increase of the compactness (circle-like shape) of the

ROI (p<0,01). A significant correlation was observed between T2 sites that are not adjacent to T1 sites and a greater amount of mineralized tissue (p<0,01).

Xenogeneic bone graft. Very similar areas of bovine bone grafts were observed between T1 and T3 at each time interval and these were significantly higher than the T2 treatment group. The area value of DBBM was significantly higher in T2 when these sites were adjacent to T1 treatment sites (figure 3.11) (Pearson correlation, p<0,05). When the proportions of graft particles were evaluated within the region of interest, they were higher for the T1 group at 2 and 6 weeks of healing as compared to T3; although this difference was not statistically significant and disappeared at the 3 months healing period. There is a trend of DBBM percentage decrease between 6 weeks and 3 months (figure 3.10).

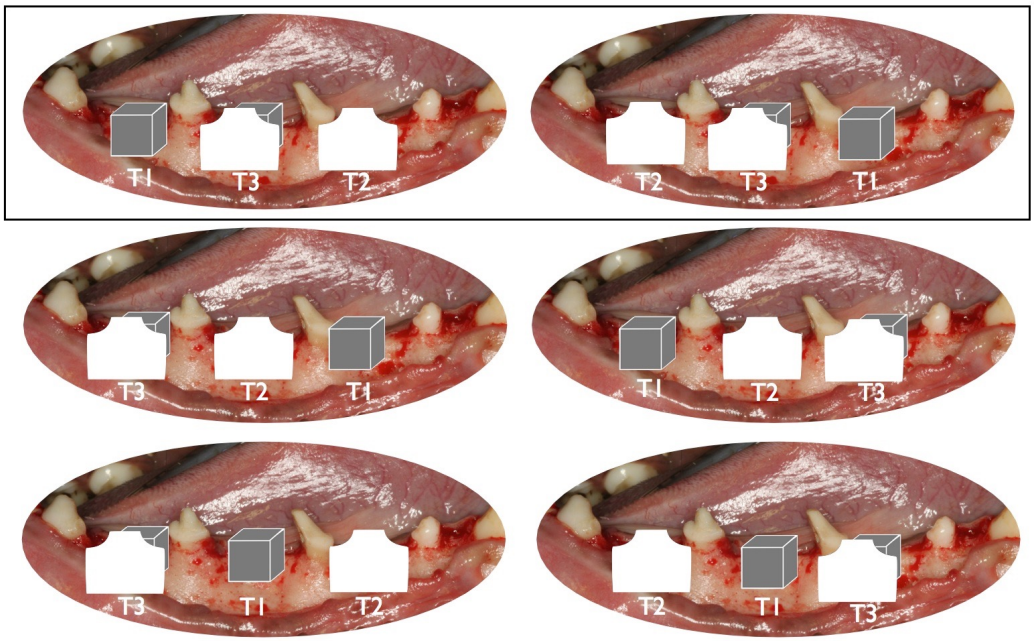

Figure 3 . 11 In this schematic illustration, out of the six random treatment dispositions, the black rectangle indicates those cases with a statistically lower DBBM quantity in T2 measured as mm^2 and a greater proportion of mineralized tissue within the region of interest. In these two situations, immediately adjacent to T2 there is only a T3 and no T1 treatment site. Treatment groups: T1 (only DBBM-C), T2: only barrier membrane (BM), T3: combined (DBBM-C + RM)

Non-mineralized tissue. The area occupied from non-mineralized tissue was not significantly different among the three treatment groups with a significant decrease over time (table 2 and figure 3.10).

In the multivariate/multilevel model, the residual variance between dogs after entering the explanatory variables was not significantly different from 0 in relation with the three outcome variables included, indicating no clustering effect at the animal level.

The analysis of the covariance in the random part of the model showed that: i) the percentage of DBBM particles was in inverse proportion with the percentage of mineralized tissue; ii) the greater the ROI, the higher the proportion of DBBM particles and iii) the greater the ROI the less the proportion of mineralized tissue.

Chapter four

Discussion

Lateral bone augmentation with guided bone regeneration is a well-documented surgical procedure that aims to augment the residual alveolar ridge, either around a surgically placed dental implant (simultaneous procedure) or before implant installation (staged procedure) (Hämmerle & Jung, 2003). Both therapeutic concepts have resulted in good clinical outcomes resulting in similar implant survival rates when comparing implants in regenerated bone versus pristine bone (Donos et al 2008). Older studies have shown the sequence of healing events leading to bone regeneration with GBR therapeutic concept (Schenk *et al*., 1994). Notwithstanding this comforting clinical data and the histological information from the classical pre-clinical studies, there is still limited information on the biological understanding of the process. It is still unknown what the clinical factors (defect, healing time) and surgical factors (use of barrier membrane, graft or combination of both) are that significantly influence this process of lateral bone augmentation. For this purpose, the relatively high number of animals used in this in vivo investigation and the complex evaluation times were a requirement to be able to collect enough reliable data on the wound healing dynamics in order to provide meaningful information.

The present study wanted to investigate the influence of the biomaterials used in GBR procedures for the treatment of horizontal bone defects in dogs. Different healing times (4 days, 2 weeks, 6 weeks, 3 months) were considered to analyze the variations in tissue composition at different time points. A multivariate/multilevel analysis was used to answer the question whether factors other than the treatment group and the healing time can be correlated to the GBR treatment outcomes.

A correlation was found between greater augmented volume, represented by the total ROI measurement, and the use of a combination of BM and DBBM (T3 treatment group). These findings highlight the relevance of the use of this combined strategy in order to provide the space and stability to the augmented area and to confirm that the space-making concept is an important requirement for GBR (Hardwick *et al*., 1995). A recent animal study tested the combination of a RM and a bone substitute and provided similar findings(Schwarz *et al*., 2010c). The authors of this study found that the GBR procedure used to treat chronic-type horizontal bone defects tended to increase the augmented area. These findings have also been corroborated clinically; a recent literature review suggested that a graft may be necessary when a non space-maintaining membrane is used (Donos *et al*., 2008).

Another important finding correlates a greater proportion of mineralized tissue with the use of the membrane alone (T2 treatment group). These findings are consistent with other pre-clinical data that demonstrated how barrier membranes significantly enhanced bone regeneration by stabilizing the underlying blood clot and preventing gingival tissue cells ingrowth into the defect (Oh *et al*., 2006). It is important to highlight that T2 groups show the smallest regenerated area, in which the proportion of mineralized tissue is bigger, but the the total volume of newly formed bone is quite the same in all treatment groups.

Longer healing time points showed a statistically significant greater proportion of mineralized tissue in all treatment groups. Another similar pre-clinical study demonstrated the validity of this finding(Schwarz *et al*., 2010c). It confirms the clinical need of a reasonable amount of time to allow the development of the bone regeneration process, from the clot formation to the late phases of bone remodeling during bone maturation.

Another relevant factor associated with new bone formation was the defect anatomy. The regression model demonstrated that both the bucco-lingual width of lingual bone plate and the horizontal bucco-lingual depth of the defect influence the outcomes in terms of greater proportion of

mineralized tissue and greater augmented area. Considering the width of the crest, we found that the higher that the bucco-lingual dimension was at the base of the defect at surgery 2, the higher the percentage of newly formed bone, independently of the treatment group. It could be speculated that a thick bone crest has a higher regenerative potential than a thin one.

Although the defects presented in our study were standardized at surgery 1, we observed at the time of surgery 2 a statistically significant difference in terms of defect depth, being M1 almost two times deeper than P2 sites. Deeper defect showed statistically better performance of the augmentation procedures. This finding confirms that a more self-contained defect favors space maintenance feature and blood clot stabilization. These results were further corroborated by the correlation between a higher defect depth and a lower percentage of non-mineralized tissue. These findings are consistent with a pre-clinical model in which the amount of new bone formation around teeth and implants depended on the baseline bucco-lingual width of the defect (Wikesjö *et al*., 2006). Clinical data from a recent literature review underlined the importance of the bone walls adjacent to the defect in the selection of the regenerative strategy (Benic & Hämmerle, 2014). Our histological findings could support this clinical recommendation.

At 3 months we observed a proportion of new mineralized tissue of 36-37% in the two treatment groups where DBBM was present (T1 and T3). A pre-clinical study that evaluated the GBR performance by means of DBBM and RM in horizontal bone dehiscence around implant showed consistent finding with our results (39% of mineralized tissue in the regenerated area after 10 weeks of healing – values calculated from the data provided in the publication)(Mihatovic *et al*., 2012). These results are not consistent with another study where the same grafting material was used (Araújo *et al*., 2010) and a higher rate of newly formed bone was observed (45% at 4 weeks). It should be considered that in the latter study, self-containing defects (fresh extraction sockets) were filled with DBBM, providing a greater regenerative potential. All these observations demonstrate the relevance of the anatomy of the residual defect to be augmented.

The atrophic ridge resulted from our experimental model may be classified as type 4 following a recent classification for horizontal augmentations (Benic & Hämmerle, 2014). The authors of this classification recommend for the treatment of type 4 defects the use of autogenous bone block as the most reliable procedure. A common finding in T1 and T3 treatment groups was an apical displacement of the DBBM particles. In another study evaluating the use of graft particles together with a BM the authors observed the same phenomenon (Schwarz *et al*., 2009). Better modalities of graft stabilization could be tested in order to avoid this shortcoming of GBR procedure by means of particulate grafts.

The lack of wound stability in the T1 treatment group is also demonstrated by the presence of DBBM-C particles in 65% of the T2 group sites. Although it may be speculated that the bovine bone particles came from both the T1 and T3 sites, a statistically significant correlation between a higher percentage of graft in T2 sites and proximity between T2 and T1 sites was observed. This correlation may suggest that the flap plus the DBBM-C does not provide a good stabilization of the wound in these non-containing horizontal bone defects and thus, the use of a barrier membrane should be advocated in these clinical situations. Furthermore, another justification that may in part explain these latter findings is related to the experimental model. The in vivo experimental dog model utilized in this study is a modification of the model first presented by Seibert and Nyman in the early nineties (Seibert & Nyman, 1990), which has been modified to mimic a single/double teeth horizontal bone deficiency in a partially edentulous human jaw (Schwarz *et al*., 2010*b*; 2010*a*; Jung *et al*., 2011) It is possible that a single root separating the defects may not provide sufficient isolation, and maybe other experimental models should be considered for future studies (Vierra *et al*., 2014).

The shape the region of interest was analysed trough the shape factors. They presented an evident correlation with the total ROI, the proportion of mineralized structure and DBBM particle. This new analysis can also be useful for its potential clinical implications: considering that the final

shape achieved by a augmentation procedure could affect cells behaviour and tissue composition, a regeneration procedure that easily allow to achieve such shapes of the augmented volume could be preferred; also development of new biomaterials could have benefits from this correlation.

In summary, within the limitations of this preclinical model, it may be concluded that bone regeneration in non-contained horizontal bone defects may be achieved by utilizing the three selected treatment strategies. Nevertheless, the factors that mainly influenced the outcomes of treatment were 1. the use of the BM and the DBBM-C to enhance the total regenerated area, 2. the use of the BM alone to enhance the amount of newly formed bone, 3. the bucco-lingual width of the base defect to enhance the amount of newly formed bone and reduce the amount of non-mineralized tissue and 4. the healing period (6 weeks and 12 weeks) to allow enough time for the regeneration process to occur.

Bibliography

Albrektsson T, Zarb G, Worthington P & Eriksson AR (1986). The long-term efficacy of currently used dental implants: a review and proposed criteria of success. *Int J Oral Maxillofac Implants* **1,** 11–25.

Aparicio C, Perales P & Rangert B (2001). Tilted implants as an alternative to maxillary sinus grafting: a clinical, radiologic, and periotest study. *Clin Implant Dent Relat Res* **3,** 39–49.

Araújo MG & Lindhe J (2005). Dimensional ridge alterations following tooth extraction. An experimental study in the dog. *J Clin Periodontol* **32,** 212–218.

Araújo MG, Liljenberg B & Lindhe J (2010). Dynamics of Bio-Oss Collagen incorporation in fresh extraction wounds: an experimental study in the dog. *Clin Oral Implants Res* **21,** 55–64.

Benic GI & Hämmerle CHF (2014). Horizontal bone augmentation by means of guided bone regeneration. *Periodontol 2000* **66,** 13–40.

Buser D, Ingimarsson S, Dula K, Lussi A, Hirt HP & Belser UC (2002). Long-term stability of osseointegrated implants in augmented bone: a 5-year prospective study in partially edentulous patients. *Int J Periodontics Restorative Dent* **22,** 109–117.

Cawood JI & Howell RA (1988). A classification of the edentulous jaws. *Int J Oral Maxillofac Surg* **17,** 232–236.

Chiapasco M & Zaniboni M (2009). Clinical outcomes of GBR procedures to correct peri-implant dehiscences and fenestrations: a systematic review. *Clin Oral Implants Res* **20 Suppl 4,** 113–123.

Chiapasco M, Abati S, Romeo E & Vogel G (1999). Clinical outcome of autogenous bone blocks or guided bone regeneration with e-PTFE membranes for the reconstruction of narrow edentulous ridges. *Clin Oral Implants Res* **10,** 278–288.

Chiapasco M, Casentini P & Zaniboni M (2009). Bone augmentation procedures in implant dentistry. *Int J Oral Maxillofac Implants* **24 Suppl,** 237–259.

Cho TJ, Gerstenfeld LC & Barnes GL (2001). Cytokines and fracture healing. *Current Opinion in Orthopedics 72,* 403–408.

Chrcanovic BR, Albrektsson T & Wennerberg A (2015). Tilted versus axially placed dental implants: A meta-analysis. *J Dent* **43,** 149–170.

Dahlin C, Linde A, Gottlow J & Nyman S (1988). Healing of bone defects by guided tissue regeneration. *Plast Reconstr Surg* **81,** 672–676.

Dahlin C, Sennerby L, Lekholm U, Linde A & Nyman S (1989). Generation of new bone around titanium implants using a membrane technique: an experimental study in rabbits. *Int J Oral Maxillofac Implants* **4,** 19–25.

Dempster DW, Compston JE, Drezner MK, Glorieux FH, Kanis JA, Malluche H, Meunier PJ, Ott SM, Recker RR & Parfitt AM (2013). Standardized nomenclature, symbols, and units for bone histomorphometry: a 2012 update of the report of the ASBMR Histomorphometry Nomenclature Committee. *J Bone Miner Res* **28,** 2–17.

Dennis SC, Berkland CJ, Bonewald LF & Detamore MS (2014). Endochondral Ossification for Enhancing Bone Regeneration: Converging Native Extracellular Matrix Biomaterials and Developmental Engineering In Vivo. *Tissue Eng Part B Rev*; E-pub ahead of print. DOI: 10.1089/ten.TEB.2014.0419.

Devescovi V, Leonardi E, Ciapetti G & Cenni E (2008). Growth factors in bone repair. *Chir Organi Mov* **92,** 161–168.

Donos N, Mardas N & Chadha V (2008). Clinical outcomes of implants following lateral bone augmentation: systematic assessment of available options (barrier membranes, bone grafts, split osteotomy). *J Clin Periodontol* **35,** 173–202.

Eckert SE & Laney WR (1989). Patient evaluation and prosthodontic treatment planning for

osseointegrated implants. *Dent Clin North Am* **33,** 599–618.

Ekelund J-A, Lindquist LW, Carlsson GE & Jemt T (2003). Implant treatment in the edentulous mandible: a prospective study on Brånemark system implants over more than 20 years. *Int J Prosthodont* **16,** 602–608.

Esposito M, Grusovin MG, Felice P, Karatzopoulos G, Worthington HV & Coulthard P (2009). Interventions for replacing missing teeth: horizontal and vertical bone augmentation techniques for dental implant treatment. *Cochrane Database Syst Rev* CD003607.

Gerstenfeld LC & Cullinane DM (2003). Fracture healing as a post-natal developmental process: Molecular, spatial, and temporal aspects of its regulation. *J Cell Biochem **88*,** 873–884.

Gilbert SF (2000). *Osteogenesis: the development of bones*, 6 edn.ed. Sinauer. Developmental Biology, Sunderland (MA).

Hardwick R, Hayes BK & Flynn C (1995). Devices for dentoalveolar regeneration: an up-to-date literature review. *J Periodontol* **66,** 495–505.

Hämmerle C, Jung RE & Feloutzis A (2002). A systematic review of the survival of implants in bone sites augmented with barrier membranes (guided bone regeneration) in partially edentulous patients. *J Clin Periodontol* **29 suppl 3**, 226–231 discussion232–3.

Hämmerle CHF & Jung RE (2003). Bone augmentation by means of barrier membranes. *Periodontol 2000* **33,** 36–53.

Hämmerle CHF, Jung RE, Yaman D & Lang NP (2008). Ridge augmentation by applying bioresorbable membranes and deproteinized bovine bone mineral: a report of twelve consecutive cases. *Clin Oral Implants Res* **19,** 19–25.

Hurley LA, Stinchfield FE, Bassett AL & Lyon WH (1959). The role of soft tissues in osteogenesis. An experimental study of canine spine fusions. *J Bone Joint Surg Am* **41-A,** 1243–1254.

Jensen SS & Terheyden H (2009). Bone augmentation procedures in localized defects in the alveolar ridge: clinical results with different bone grafts and bone-substitute materials. *Int J Oral Maxillofac Implants* **24 Suppl,** 218–236.

Jung RE, Fenner N, Hämmerle CHF & Zitzmann NU (2013). Long-term outcome of implants placed with guided bone regeneration (GBR) using resorbable and non-resorbable membranes after 12-14 years. *Clin Oral Implants Res* **24,** 1065–1073.

Jung RE, Kokovic V, Jurisic M, Yaman D, Subramani K & Weber FE (2011). Guided bone regeneration with a synthetic biodegradable membrane: a comparative study in dogs. *Clin Oral Implants Res* **22,** 802–807.

Kaigler D, Avila-Ortiz G, Travan S, Taut AD, Padial-Molina M, Rudek I, Wang F, Lanis A & Giannobile WV (2015). Bone engineering of maxillary sinus bone deficiencies using enriched CD90+ stem cell therapy: A randomized clinical trial. *J Bone Miner Res*; e-pub ahead of print DOI: 10.1002/jbmr.2464.

Kaigler D, Cirelli JA & Giannobile WV (2006). Growth factor delivery for oral and periodontal tissue engineering. *Expert Opin Drug Deliv* **3,** 647–662.

Kalfas IH (2001). Principles of bone healing. *Neurosurg Focus* **10,** E1.

Lekholm U, Gröndahl K & Jemt T (2006). Outcome of oral implant treatment in partially edentulous jaws followed 20 years in clinical function. *Clin Implant Dent Relat Res* **8,** 178–186.

McAllister BS & Haghighat K (2007). Bone augmentation techniques. *J Periodontol* **78,** 377–396.

Meijer GJ, de Bruijn JD, Koole R & van Blitterswijk CA (2008). Cell based bone tissue engineering in jaw defects. *Biomaterials* **29,** 3053–3061.

Melcher AH (1976). On the repair potential of periodontal tissues. *J Periodontol* **47,** 256–260.

Mihatovic I, Becker J, Golubovic V, Hegewald A & Schwarz F (2012). Influence of two barrier membranes on staged guided bone regeneration and osseointegration of titanium implants in dogs.

Part 2: augmentation using bone graft substitutes. *Clin Oral Implants Res* **23,** 308–315.

Mojon P, Thomason JM & Walls AWG (2004). The impact of falling rates of edentulism. *Int J Prosthodont* **17,** 434–440.

Monje A, Fu J-H, Chan H-L, Suarez F, Galindo-Moreno P, Catena A & Wang H-L (2013). Do implant length and width matter for short dental implants (. *J Periodontol* **84,** 1783–1791.

Nauth A, Ristevski B, Li R & Schemitsch EH (2011). Growth factors and bone regeneration: how much bone can we expect? *Injury* **42,** 574–579.

Neldam CA & Pinholt EM (2012). State of the art of short dental implants: a systematic review of the literature. *Clin Implant Dent Relat Res* **14,** 622–632.

Nevins M, Mellonig JT, Clem DS, Reiser GM & Buser DA (1998). Implants in regenerated bone: long-term survival. *Int J Periodontics Restorative Dent* **18,** 34–45.

Nyman S, Gottlow J, Karring T & Lindhe J (1982). The regenerative potential of the periodontal ligament. An experimental study in the monkey. *J Clin Periodontol* **9,** 257–265.

Oh S-H, Kim Y, Park J-Y, Jung YJ, Kim S-K & Park S-Y (2014). Comparison of fixed implant-supported prostheses, removable implant-supported prostheses, and complete dentures: patient satisfaction and oral health-related quality of life. *Clin Oral Implants Res*; e-pub ahead of print DOI: 10.1111/clr.12514.

Oh S-H, Kim JH, Kim JM & Lee JH (2006). Asymmetrically porous PLGA/Pluronic F127 membrane for effective guided bone regeneration. *J Biomater Sci Polym Ed* **17,** 1375–1387.

Olson E (2011). Particle Shape Factors and Their Use in Image Analysis Part 1: Theory. *Journal of GXP Compliance* **15,** 85.

Pjetursson BE, Thoma D, Jung R, Zwahlen M & Zembic A (2012). A systematic review of the survival and complication rates of implant-supported fixed dental prostheses (FDPs) after a mean observation period of at least 5 years. *Clin Oral Implants Res* **23 Suppl 6,** 22–38.

Preciado A, Del Río J, Suárez-García M-J, Montero J, Lynch CD & Castillo-Oyagüe R (2012). Differences in impact of patient and prosthetic characteristics on oral health-related quality of life among implant-retained overdenture wearers. *J Dent* **40,** 857–865.

Rasia-dal Polo M, Poli P-P, Rancitelli D, Beretta M & Maiorana C (2014). Alveolar ridge reconstruction with titanium meshes: a systematic review of the literature. *Med Oral Patol Oral Cir Bucal* **19,** e639–e646.

Rocchietta I, Fontana F & Simion M (2008). Clinical outcomes of vertical bone augmentation to enable dental implant placement: a systematic review. *J Clin Periodontol* **35,** 203–215.

Ronda M, Rebaudi A, Torelli L & Stacchi C (2014). Expanded vs. dense polytetrafluoroethylene membranes in vertical ridge augmentation around dental implants: a prospective randomized controlled clinical trial. *Clin Oral Implants Res* **25,** 859–866.

Schenk RK, Buser D, Hardwick WR & Dahlin C (1994). Healing pattern of bone regeneration in membrane-protected defects: a histologic study in the canine mandible. *Int J Oral Maxillofac Implants* **9,** 13–29.

Schlegel AK, Möhler H, Busch F & Mehl A (1997). Preclinical and clinical studies of a collagen membrane (Bio-Gide). *Biomaterials* **18,** 535–538.

Schwarz F, Ferrari D, Balic E, Buser D, Becker J & Sager M (2010*a*). Lateral ridge augmentation using equine- and bovine-derived cancellous bone blocks: a feasibility study in dogs. *Clin Oral Implants Res* **21,** 904–912.

Schwarz F, Ferrari D, Podolsky L, Mihatovic I & Becker J (2010*b*). Initial pattern of angiogenesis and bone formation following lateral ridge augmentation using rhPDGF and guided bone regeneration: an immunohistochemical study in dogs. *Clin Oral Implants Res* **21,** 90–99.

Schwarz F, Jung RE, Fienitz T, Wieland M, Becker J & Sager M (2010c). Impact of guided bone regeneration and defect dimension on wound healing at chemically modified hydrophilic titanium implant surfaces: an experimental study in dogs. *Journal of Clinical periodontology* **37,**

474–485.

Schwarz F, Sager M, Ferrari D, Mihatovic I & Becker J (2009). Influence of recombinant human platelet-derived growth factor on lateral ridge augmentation using biphasic calcium phosphate and guided bone regeneration: a histomorphometric study in dogs. *J Periodontol* **80,** 1315–1323.

Seibert J & Nyman S (1990). Localized ridge augmentation in dogs: a pilot study using membranes and hydroxyapatite. *J Periodontol* **61,** 157–165.

Simion M, Jovanovic SA, Tinti C & Benfenati SP (2001). Long-term evaluation of osseointegrated implants inserted at the time or after vertical ridge augmentation. A retrospective study on 123 implants with 1-5 year follow-up. *Clin Oral Implants Res* **12,** 35–45.

Tinti C, Parma-Benfenati S & Polizzi G (1996). Vertical ridge augmentation: what is the limit? *Int J Periodontics Restorative Dent* **16,** 220–229.

Tonetti MS, Hämmerle CHFEuropean Workshop on Periodontology Group C (2008). Advances in bone augmentation to enable dental implant placement: Consensus Report of the Sixth European Workshop on Periodontology. *Journal of clinical periodontology*.

Urban IA, Lozada JL, Jovanovic SA, Nagursky H & Nagy K (2014). Vertical ridge augmentation with titanium-reinforced, dense-PTFE membranes and a combination of particulated autogenous bone and anorganic bovine bone-derived mineral: a prospective case series in 19 patients. *Int J Oral Maxillofac Implants* **29,** 185–193.

Vierra M, Mau LP, Huynh-Ba G, Schoolfield J & Cochran DL (2014). A lateral ridge augmentation study to evaluate a synthetic membrane for guided bone regeneration: an experiment in the canine mandible. *Clin Oral Implants Res*; e-pub ahead of print DOI: 10.1111/clr.12517.

Vignoletti F & Abrahamsson I (2012). Quality of reporting of experimental research in implant dentistry. Critical aspects in design, outcome assessment and model validation. *J Clin Periodontol* **39 Suppl 12,** 6–27.

Wang HL & Boyapati L (2006). "PASS" principles for predictable bone regeneration. *Implant Dent*.

Wikesjö UME, Susin C, Qahash M, Polimeni G, Leknes KN, Shanaman RH, Prasad HS, Rohrer MD & Hall J (2006). The critical-size supraalveolar peri-implant defect model: characteristics and use. *J Clin Periodontol* **33,** 846–854.

Zitzmann NU, Margolin MD, Filippi A, Weiger R & Krastl G (2008). Patient assessment and diagnosis in implant treatment. *Aust Dent J* **53 Suppl 1,** S3–S10.